

Unified collision model of coherent and measurement-based quantum feedbackAlfred Harwood ¹, Matteo Brunelli ², and Alessio Serafini¹¹*Department of Physics & Astronomy, University College London, Gower Street, WC1E 6BT, London, United Kingdom*²*Department of Physics, University of Basel, Klingelbergstrasse 82, 4056 Basel, Switzerland*

(Received 6 April 2022; accepted 18 September 2023; published 16 October 2023)

We introduce a general framework, based on collision models and discrete completely positive maps, to describe on an equal footing coherent and measurement-based feedback control of quantum mechanical systems. We apply our framework to prominent tasks in quantum control, ranging from cooling to Hamiltonian control. Unlike other proposed comparisons, where coherent feedback always proves superior, we find that either measurements or coherent manipulations of the controller can be advantageous depending on the task at hand. Measurement-based feedback is typically superior in cooling, while coherent feedback is better at assisting quantum operations. Furthermore, we show that both coherent and measurement-based feedback loops allow one to simulate arbitrary Hamiltonian evolutions, and discuss their respective effectiveness in this regard.

DOI: [10.1103/PhysRevA.108.042413](https://doi.org/10.1103/PhysRevA.108.042413)**I. TWO FLAVORS OF QUANTUM FEEDBACK CONTROL**

The designation “coherent feedback” (CF) is used to describe a broad class of quantum control strategies where the controller (an auxiliary system that interacts with the main system for the purpose of steering it toward desired targets) processes only quantum information. CF can be contrasted with “measurement-based feedback” (MF), in which the controller processes classical information resulting from measurement outcomes. The theory of MF goes back to the work of Belavkin [1], while CF has its origins in the “all-optical feedback” [2,3], based on the input-output formalism [4]. There, the output from a cavity is used to modulate the cavity’s dynamics (without measurements being performed) and the process has a clear, directional “feedback loop” structure. Later, with the advent of quantum information, the term “coherent quantum feedback” was used to describe general interactions between two quantum systems aimed at control tasks [5,6]. In our work, we focus on the former definition involving explicit loops, as will be made clear. MF has long been used for achieving quantum control [7–10] and CF has recently emerged as a powerful alternative with applications in quantum optics [11–13], optomechanics [14–20], nanomechanics [21], NV centers [22], and circuit QED setups [23–25].

Both strategies have been widely studied theoretically, especially in the arena of quantum optics [2,3,9,11,16,26–30]. It is often claimed that CF is inherently superior to MF, and for certain definitions, regimes, and problems, this is the case [6,11,26,27]. However, other results suggest a less clear-cut scenario and point at the usefulness of quantum measurements [29], which can even outperform CF, e.g., in stabilizing the squeezing of a cavity mode [31]. In particular,

the alleged superiority of CF often hinges on comparisons with measurement-based unconditional, averaged dynamics without considering the corresponding conditional dynamics, whose stochastic jumps cannot be reproduced by unitary means (a way to express the notorious measurement problem), or misses the potential of nondestructive quantum measurements, upon which system and controller evolve according to the von Neumann postulate and then may interact with each other once again afterwards. A broader approach is then required to fully take into account the possibilities offered by quantum measurements.

To this aim, we present a unified framework for describing coherent and measurement-based feedback loops as cascaded collision models. Collision models (CMs) are a class of schemes for modeling open quantum dynamics where the system repeatedly interacts with an environment, which is refreshed after each interaction [32–36]. They have found widespread application in quantum thermodynamics [37–40], quantum optics [41], non-Markovian quantum systems [42–45], and have also been applied to a discretized model for CF, encompassing an exhaustive treatment of delays [30]. Another treatment of quantum feedback with discrete, repeated interactions may be found in [46].

We put forward a general framework of quantum feedback by treating the environment of the collision model as a “controller” that undergoes *two* sequential interactions with the system before being refreshed. In-between these two interactions, the controller is processed, either through measurements (in MF), or coherently (in CF). Note that, at variance with some previous treatments, such as [47], we assume the system cannot be manipulated or measured directly, but only indirectly through the controller whose coupling to the system is fixed, unlike, e.g., in [48]. If the system is subject to additional noise, we assume that the controller does not have access to its source (as would be the case in quantum feedforward, according to a distinction made in [6]).

Our model allows for a fair comparison between MF and CF since the system noise, controller state, and

Published by the American Physical Society under the terms of the Creative Commons Attribution 4.0 International license. Further distribution of this work must maintain attribution to the author(s) and the published article’s title, journal citation, and DOI.

Appendix D 2 b, where it is applied to the optimization of an operator control task. Let us also remark that, under certain conditions, in “forgetful” MF schemes, i.e., without access to the measurement record, the feedback action results in a deterministic CP map and MF reverts, so to speak, to CF, as exemplified in [64].

In the remainder of this work, we shall take system and controller to have the same Hilbert space dimension d and both couplings U_1 and U_2 to be partial swaps, as commonly used in CMs [35,66,67], i.e., we set $U_s = \sqrt{\tau}\mathbb{1} - i\sqrt{1-\tau}\hat{S}$, where \hat{S} is the unitary swap operator and $0 \leq \tau \leq 1$ is the transmissivity. It is easy to see that such an interaction is generated by the swap operator itself, which is clearly Hermitian. For qubits, this evolution corresponds to the Heisenberg coupling $\sigma_x^{(1)}\sigma_x^{(2)} + \sigma_y^{(1)}\sigma_y^{(2)} + \sigma_z^{(1)}\sigma_z^{(2)}$, where $\sigma_w^{(j)}$ denotes the Pauli matrix w acting on a hypothetical qubit system j . In practice, this interaction occurs naturally among spins but is typically nontrivial to obtain in quantum optics because it requires the engineering of equally weighted exchange ($\sigma_+^{(1)}\sigma_-^{(2)} + \text{H.c.}$) and dispersive ($\sigma_z^{(1)}\sigma_z^{(2)}$) interactions. Nevertheless, we adopt partial swaps here because they mimic coherent, beam-splitter interactions in optics and, crucially, allow for a very straightforward generalization to any dimension d . Many (though not all, as will be noted in due course) of our quantitative results depend on such a choice and it will be interesting to investigate other couplings, such as exchange ones (which share salient features with partial swaps, such as the conservation of the total number of excitations) in future work.

III. FEEDBACK COOLING

First, we apply our framework to the task of feedback cooling, considering both noisy and clean controllers, as we explain in the following. In this section, we also assume that the noise due the inaccessible environmental degrees of freedom, represented by the CP map \mathcal{E} , takes the form of a depolarizing channel acting on the system as $\mathcal{E}(\rho) = \lambda\rho + (1-\lambda)\frac{1}{d}\mathbb{1}$ where λ determines the strength of such noise and $\mathbb{1}$ is the identity operator with dimension determined by the context.

A. Noisy controller

In this section, we consider the case where the controller is in the maximally mixed, or infinite temperature, state $\eta = \frac{1}{d}\mathbb{1}$, which we refer to as a “noisy controller” (notice in fact that the noise acting on the system also comprises the “unaccessible” depolarizing channel). The relevant figure of merit to cooling is the von Neumann entropy of the steady state of the system (i.e., a state which is unchanged by the application of a single iteration of the MF or CF protocol). If the steady state exists and is unique (as will be the case in our examples), any input will tend to the steady state upon repeated applications of the protocol.

For CF, the set of allowed in-loop operations on the controller is the set of single-qudit unitaries. It is shown in Appendix B 1, by virtue of the subadditivity of entropy, that CF is incapable of counteracting the noise on the system and leads to a maximally mixed steady state $\rho_S = \frac{1}{d}\mathbb{1}$. Notice

that this is the case *regardless of the choice of interaction unitary* U .

For MF, we consider a protocol with an in-loop projective measurement in an arbitrary basis $\{|j\rangle, j = 0, \dots, d-1\}$. Let us consider a strategy where, after measuring, a unitary is applied to the controller which maps all postmeasurement states to the same pure state, which we will label $|0\rangle$ (the wisdom of this choice will be justified shortly). Upon averaging on the measurement results, the system reaches the so-called “unconditional” steady state, evaluated in Appendix B 2 a as

$$\rho_S = \frac{1}{d} \frac{d(1-\tau) + \tau - \lambda\tau^2}{1 - \lambda\tau^2} |0\rangle\langle 0| + \sum_{j=1}^{d-1} \frac{1}{d} \frac{\tau - \lambda\tau^2}{1 - \lambda\tau^2} |j\rangle\langle j|, \quad (1)$$

whose entropy is clearly lower than the maximally mixed state for all parameter values except for the trivial case where $\tau = 1$ and the system and controller do not interact. Thus, we have shown that introducing measurements into the feedback loop is advantageous. If a cold environment (in the form of a pure controller) is not available as a resource, MF outperforms all possible CF protocols in the limit of high controller’s temperatures, as measurement acts as a powerful tool for preparing the controller’s state, which cannot be reproduced through unitary means.

By applying an entropy power inequality [68,69], in Appendix B 2 b it is proven that, for an input diagonal in the measurement basis (as is the case for the maximally mixed state), the entropy of the *conditional* output state is minimized when, after measuring the controller, all measurement outcomes are mapped to the system’s dominant eigenvector (corresponding to the system state’s largest eigenvalue). Furthermore, when the input is diagonal in the measurement basis, the output is diagonal in the same basis, with the same dominant eigenvector. Thus, for repeated application, starting with a maximally mixed input (or any input state with dominant eigenvector $|0\rangle$) our MF protocol is optimal when considering conditional dynamics. We could not prove its optimality for unconditional dynamics too, although it is confirmed by all numerical evidence we possess.

In general, conditional MF does not yield a steady state, resulting in oscillating entropies (see Fig. 2). Only in the case of a full swap ($\tau = 0$) can the postmeasurement unitary completely undo the stochasticity of the measurement, leading to the steady state $|0\rangle$, i.e., to perfect cooling. Examining Fig. 2 one can see that the cooling performance decreases with τ (as lower τ imply the possibility of injecting low-entropy states from the controller) and, as one should expect, decreases with the noise strength λ (see Appendix B 2 a). Observe also that the entropy “jumps” become larger for higher system dimensions. This study also allows us to estimate the cooling rate of the model, i.e., the typical number of iterations needed to approach the unconditional entropy, as $1/(1-\tau)$ (in that the interaction with the controller dominates the cooling process). Let us note in passing that this scenario is tightly reminiscent of the juxtaposition between standard (“measurement-based”) and unitary (“autonomous”) Maxwell demons [70–74].

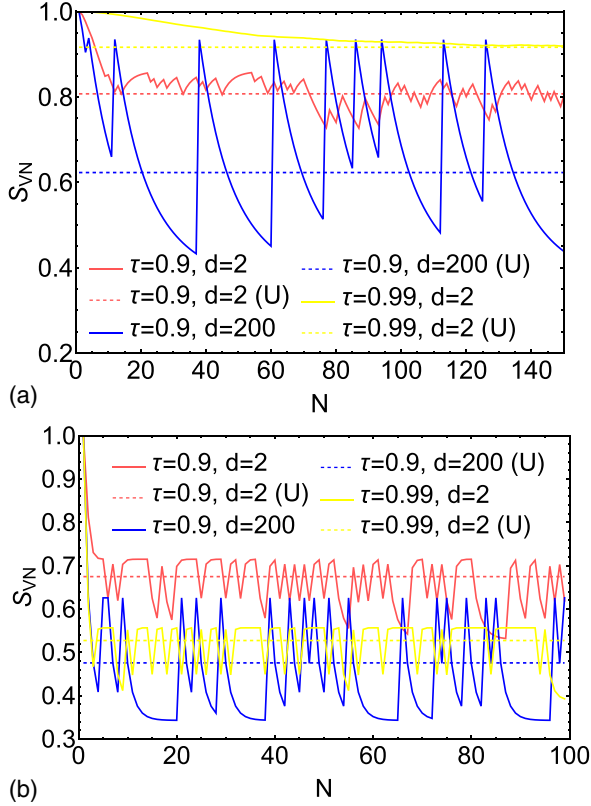


FIG. 2. Normalized (with base- d logarithms) von Neumann entropy of conditional (continuous lines) and steady-state unconditional (horizontal dotted lines) measurement-based feedback cooling for a maximally mixed initial state at different values of τ and d ; $\lambda = 0.99$ in the top graph (a) and $\lambda = 0.9$ in the bottom one (b). The x axes report the number of iterations.

B. Clean controller

While MF outperforms CF when cooling with a maximally mixed controller, this is not always the case when the controller is “clean,” i.e., initialized in a pure state $\eta = |0\rangle\langle 0|$ (note that this is the case, for instance, when the controller is a light mode at room temperature, like in sideband cooling). For CF, we consider the case where the in-loop unitary is the identity (which, as proven in Appendix B 3, is optimal for qubits assuming $|0\rangle$ is an eigenvector of the steady state) while for MF we consider the protocol from the previous section, which was optimal for a noisy controller. In this case too, we have found no strategies capable of improving on these two choices.

In both cases, we find that the steady states have one eigenvalue larger than the others, which are degenerate. For states like these, both the linear and von Neumann entropies are solely functions of the largest eigenvalue and are therefore equivalent for the purposes of comparison. Here, we present the linear entropies for qubit systems in view of their more compact expressions (more general expressions for arbitrary dimension can be found in Appendixes B 3 and B 4). The steady-state linear entropy for the MF protocol is

$$S_{\text{MF}} = \frac{1}{2} - \frac{(\tau^2 - 1)^2}{2(\tau^2\lambda - 1)^2}, \quad (2)$$

while for the CF protocol one has

$$S_{\text{CF}} = \frac{1}{2} - \frac{8\tau^2(\tau - 1)^2}{((1 - 2\tau)^2\lambda - 1)^2}. \quad (3)$$

Comparing the two steady-state entropies for qubits (see Appendix B 4), we find that $S_{\text{MF}} < S_{\text{CF}}$ for $\tau < \frac{1}{3}$ and $S_{\text{MF}} > S_{\text{CF}}$ for $\tau > \frac{1}{3}$. Thus, there are two regimes: one where MF outperforms CF and one where CF outperforms MF. We also find that when $\tau = \frac{1}{2}$, $S_{\text{CF}} = 0$ and CF is able to stabilize a pure state, but no MF protocol with projective measurements can stabilize a pure state for $\tau = \frac{1}{2}$ (see Appendix B 4). Conversely, for $\tau = 0$, MF is always capable of stabilizing a pure state while CF cannot stabilize any state other than the maximally mixed state, as the action of a unitary alone cannot undo the effect of the depolarizing map.

C. Finite-temperature controller

At intermediate controller noises (where the controller is neither pure nor maximally mixed), we have compared the heuristically optimized protocols where MF prepares the state corresponding to the largest eigenvalue of the controller, while the CF loop applies the in-loop identity. Plots of specific case studies may be found in Appendix B 5. As a significant example, for $d = 2$, $\tau = 0.5$, and $\lambda = 0.25$, MF exhibits a superior cooling performance for all controller noises (i.e., all values of the controller’s largest eigenvalue). Significantly, a qualitative picture emerges whereby for low-temperature controllers and weak couplings the act of measurement disturbs the coherent process responsible for low-entropy environmental states to be transferred to the system, thus making MF inferior to CF. On the other hand, with strong couplings and noisy environments, the purification from the act of measurement compensates for this and allows for the injection of purer states, so that MF then tends to perform better than CF under such circumstances.

IV. EXCITATION PRESERVATION

After a task based on entropy, we now consider one focused on the system’s energy. We consider a qubit initially prepared in the excited state $|1\rangle$ (with $|0\rangle$ being the ground state) subject to decay, modeled by \mathcal{E} with Kraus operators $E_0 = \sqrt{\gamma}|0\rangle\langle 1|$, $E_1 = \sqrt{1 - \gamma}|1\rangle\langle 1| + |0\rangle\langle 0|$. We assume a controller initialized in the maximally mixed state, employ a feedback loop, either CF or MF based, to counter the effect of decay and adopt the steady-state occupation of the $|1\rangle$ state as our figure of merit.

A. Coherent feedback

For CF, we restrict the in-loop unitaries to rotations $U = \cos \chi \mathbb{1} + i \sin \chi \sigma_y$ and optimize the protocol numerically, finding that the optimal CF protocol depends on the partial swap strength; for $\tau > \frac{1}{2}$ ($\tau < \frac{1}{2}$), the optimal setting is $\chi = 0$ ($\chi = \frac{\pi}{2}$) (see Appendix C 1 for more details).

Figure 3(a) shows the performance of the setup with weak damping, characterized by $\gamma = 0.2$ and Fig. 3(b) shows the performance of the same setup with stronger damping, characterized by $\gamma = 0.8$. For $\tau > \frac{1}{2}$, increasing the noise decreases the steady-state occupation of the excited state. However,

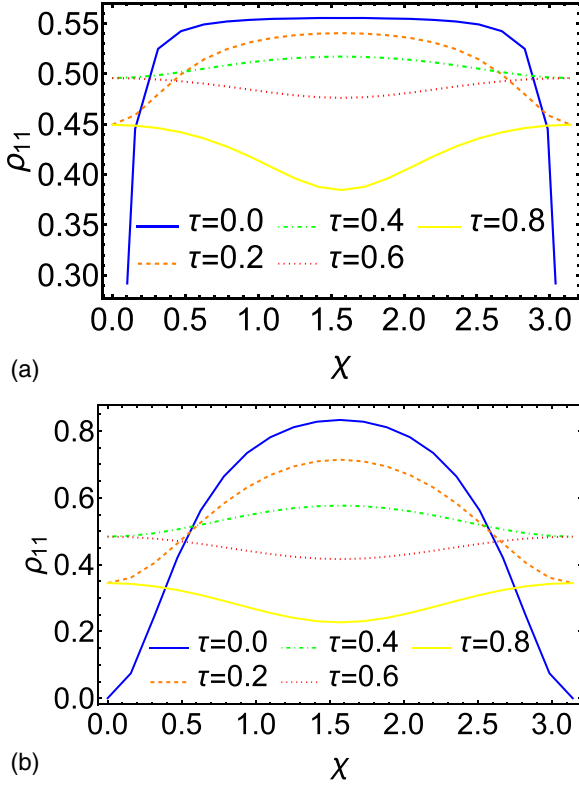


FIG. 3. The steady-state occupation of the $|1\rangle$ state for CF setups with different coupling strengths, characterized by τ . (a) For a setup with amplitude damping characterized by $\gamma = 0.2$ and (b) is for a setup characterized by $\gamma = 0.8$. Note that, for strong couplings ($\tau < \frac{1}{2}$), the setup with stronger amplitude damping actually has a *higher* excited-state occupation.

for strong system-controller interactions $\tau < \frac{1}{2}$, the optimal performance (when $\chi = \frac{\pi}{2}$) is *improved* by stronger damping since the action of the in-loop $\frac{\pi}{2}$ rotation is more effective at populating the $|1\rangle$ state when more of the state is initially prepared in the $|0\rangle$ state. In this sense, CF allows for the purifying effect of the amplitude damping to be harnessed for the purpose of increasing the excited-state population.

When $\chi = 0$ and the in-loop unitary is the identity, the steady-state occupation of the excited state is

$$\rho_{11}^{\chi=0} = \frac{2\tau(1-\tau)}{4(\tau-1)(\gamma-1)\tau + \gamma}, \quad (4)$$

which is a decreasing function of γ for $\tau > \frac{1}{2}$. Conversely, when $\chi = \frac{\pi}{2}$, the steady-state occupation is

$$\rho_{11}^{\chi=\frac{\pi}{2}} = \frac{1-\tau}{2(\gamma-1)\tau - \gamma + 2}, \quad (5)$$

which is an increasing function of γ for $\tau < \frac{1}{2}$.

B. Measurement-based feedback

We compare this to an intuitive MF protocol which measures the controller in the $\{|1\rangle, |0\rangle\}$ basis, does nothing if the result is $|1\rangle$, and applies an in-loop rotation with $\chi = \frac{\pi}{2}$ if the

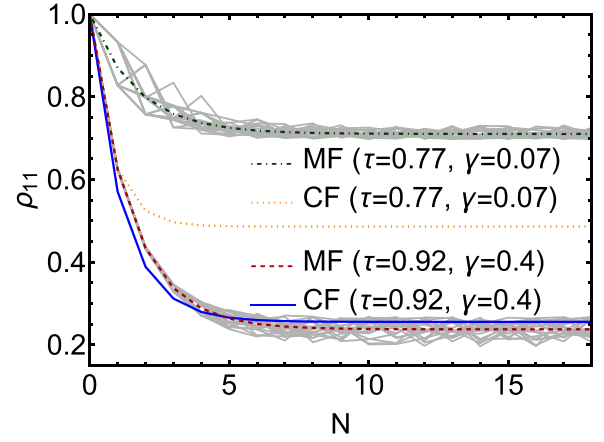


FIG. 4. Excited-state occupation against number of iterations of MF or CF. The MF trajectories shown as dark (dashed and dotted-dashed) lines are the unconditional trajectories. For each setup 50 conditional, filtered MF trajectories are shown as solid light gray lines.

result is $|0\rangle$. The excited steady-state occupation is then

$$\rho_{11}^{\text{MF}} = \frac{2 - \tau^2 - \tau}{2(\gamma - 1)\tau^2 + 2}, \quad (6)$$

which is greater than (5) for all values of τ and γ , so that MF outperforms CF in the regime of strong system-controller coupling $\tau < \frac{1}{2}$. However, for some high values of τ , (4) is greater than (6) and CF outperforms MF, though numerical investigations suggest that the advantage is small (see Appendix C 2 for further details).

Conversely, in the regime where MF outperforms CF, the advantage is larger. Figure 4 shows the occupation of the excited state against the number of feedback loop iterations.

V. OPERATOR CONTROL

Let us now turn to operator control, where the objective is to realize a certain system dynamics (possibly a “gate”) on arbitrary initial states, rather than steering the system to a certain target state.

A. Bit flipping

As an operator control task, we consider the implementation of a bit-flip operation on a qubit system ($d = 2$); we stress that the bit flip must be induced on the system by only acting on the controller. We allow in-loop operations to be any single-qubit unitary, assume that the system is not subject to additional noise (i.e., the map \mathcal{E} is the identity), and that the controller is initialized to a generic mixed state $\eta = \eta_0 |0\rangle\langle 0| + (1 - \eta_0) |1\rangle\langle 1|$. The system input state is of the general form $|\psi\rangle = \cos \frac{\chi}{2} |0\rangle + e^{i\phi} \sin \frac{\chi}{2} |1\rangle$ and the figure of merit will be the Haar-averaged fidelity of the output state to the desired state, i.e., $A = (4\pi)^{-1} \int d\phi d\chi \sin \chi \langle \psi_X | \rho_S^{\text{out}} | \psi_X \rangle$, where $|\psi_X\rangle = \sigma_x |\psi\rangle$. Crucially, the feedback protocol must be implemented without knowledge of the input state (i.e., without knowledge of χ and ϕ).

First, we consider an intuitive CF protocol, where the in-loop operation performed is a σ_x unitary. When the state $|\psi\rangle$ is put through this protocol, we obtain, as detailed in Appendix D 1, the average output fidelity for coherent feedback

$$A_{\text{CF}} = 1 - \frac{2}{3}\tau. \quad (7)$$

As shown in Appendix D 2, by using proper matrix decompositions we could fully analytically optimize our MF protocol and, quite remarkably, prove that *no MF protocol can outperform this CF protocol*. This was first proven for projective measurements, where, after interacting through the partial swap, the controller is measured in the $\{|0\rangle, |1\rangle\}$ basis (notice that all choices of basis are equivalent due to the unitary covariance of the Haar measure) and then subject to a σ_x gate, which is shown to yield maximum output fidelity $A_{\text{MF}} = \frac{2}{3} - \frac{1}{3}\tau$ regardless of the measurement outcome. This average fidelity is always smaller than what is achievable through CF (except for the trivial case $\tau = 1$). Finally, by adopting the unified description of feedback obtainable via the polar decomposition of the POVM's Kraus operators, we were able to show that the performance of MF improves with (nonprojective) weaker measurements but cannot ever outperform the CF value above for *any* in-loop POVM. Therefore, we can state that CF is definitely superior to MF in assisting bit flipping.

B. Unitary operator control in the limit of weak interactions

Having considered the task of implementing a specific unitary, we now investigate the realization of an arbitrary unitary on the system in the limit of infinitesimally weak system-controller interactions, i.e., letting $\theta \rightarrow d\theta$ in the transmissivity of the partial swap $\tau = \cos^2\theta$. To first order in $d\theta$, one finds (see Appendix E) that one iteration of MF or CF results in the following transformation on the system density operator:

$$\rho_S \rightarrow \rho_S - i[(\Lambda_j(\eta) + \eta), \rho_S]d\theta, \quad (8)$$

where Λ_j represents the particular CP map applied in loop (unitary for CF and measurement followed by a unitary for MF) from the set of possible in-loop CP maps $\{\Lambda_j\}$. Therefore, in this weak interaction limit, the system evolves unitarily for both MF and CF, under the transformation $V_j = e^{-iH_j dt}$, with $H_j = [\Lambda_j(\eta) + \eta]$. By iteratively applying this process, both MF and CF can simulate any Hamiltonian on the system, provided that it falls within the algebra generated by commutation of elements of the set $\{\Lambda_j(\eta) + \eta\}$ (assuming that the Λ_j can be changed after each iteration as necessary). If the set of in-loop CP maps generated by MF or CF is nontrivial, this algebra is typically the entire space of Hermitian matrices since all pairs of Hermitian matrices, except a set of measure zero, can generate the entire space of Hermitian matrices by commutation [75]. Thus, in the weak interaction limit, provided that the set $\{\Lambda_j(\eta) + \eta\}$ is nontrivial, both MF and CF can be used to simulate the effect of any Hamiltonian on the system and for this purpose are equivalent. However, the dramatic ability of measurements to change the

controller's spectrum can be leveraged here to achieve faster evolutions to target states than in CF schemes, as $\Lambda_j(\eta)$ can in principle be any quantum state in MF. In this regard, let us also notice that in the limiting case where η is maximally mixed, the set $\{\Lambda_j(\eta) + \eta\}$ for CF will contain only one element which will be proportional to the identity (since the action of any unitary leaves the identity unchanged), and so CF will not be able to exert any Hamiltonian control in that case.

VI. CONCLUDING REMARKS

We have introduced a common framework for coherent and measurement-based quantum feedback based on a collision model, featuring repeated interactions with an environment that acts as a controller. This allows MF and CF to be compared on equal footing, under the assumption of nondestructive measurements, so that our extensive case studies, covering a wide range of control scenarios based on partial swap interactions, provide one with strong indications of the advantages and disadvantages of each type of feedback.

At variance with what one might expect, the comparison and respective optimality of measurement-based vs coherent feedback loops is necessarily nuanced, even for fixed figures of merit, as it depends on specifics of the uncontrolled dynamics. Nonetheless, by applying our model we were able to reach a number of clear-cut results in this regard. First, we found that MF is superior to CF for the task of lowering the steady-state entropy of a system subject to noise, unless the controller is initially at very low entropy. For the case of maximum environmental entropy, we could prove exactly that CF cannot help at all, regardless of the choice of unitary interaction between system and environmental, whereas MF can still be very effective. When the controller is initialized to a pure state, the comparison becomes more subtle and the question of which type of feedback is superior depends on the strength of the interaction, as parametrized by the transmissivity τ . We showed that, in this setup, when $\tau = \frac{1}{2}$, CF can stabilize a pure state, which is not possible through any MF protocol. In contrast, when $\tau = 0$ and the interaction is as strong as it can be, we showed that MF is capable of stabilizing a pure state when CF could only stabilize the maximally mixed state. We then considered the preservation of energy in a system subject to decay, and observed that MF would prove superior to CF at strong system-controller couplings, and vice versa at weak couplings. Hence, we turned to operator control and found that CF is superior to MF for implementing a bit-flip operation on an unknown, arbitrary input state. Furthermore, we showed that MF and CF are, in most cases, equally capable of emulating any Hamiltonian on the system in the limit of weak system-controller couplings, except for maximally mixed controllers, where MF is superior since a measurement is needed to achieve any Hamiltonian engineering.

Notably, our approach is applicable to very general interactions and noises, in order to obtain optimized feedback loops for concrete setups, which will be the subject of future work, with especial regard to engineering remote Hamiltonian interactions [55] and setups based on giant emitters [58,59].

ACKNOWLEDGMENTS

M.B. acknowledges funding from the Swiss National Science Foundation (Grant No. PCEFP2_194268). We also thank F. Ciccarello for several useful discussions on collision models.

APPENDIX A: REPRODUCTION OF STANDARD FEEDBACK MODELS

This section is meant to substantiate the claim that our general framework subsumes most standard open-system treatments of feedback scenarios. More specifically, we will show that widely adopted stochastic master equations in the presence of Markovian noise and monitoring are included in our framework and, for the case of CF, provide the reader with an explicit derivation of the standard quantum optical master equation under “all-optical” coherent feedback (the true staple of the genre).

As for MF, it is straightforward to see that the monitoring and feedback actions described through stochastic master equations are encompassed by our framework through the following argument. In the continuous-time limit of infinitesimal increments, one can treat our dynamics by rearranging the four steps of each iterative cycle [(i) first interaction, (ii) measurement, (iii) CP map on the environment, (iv) second interaction] in the order [(i) first interaction, (ii) second interaction, (iii) measurement, (iv) CP map on the environment] and, by keeping the same interaction Hamiltonian in the first and second steps, by reducing it to the standard three steps process [(i) interaction, (ii) measurement, (iii) CP map on the environment], up to a mere rescaling of the interaction Hamiltonian by a factor 2. This is the standard framework for the derivation of stochastic master equations with and without feedback (see, e.g., [9,76]; see also [35] for a derivation of a master equation for collisional models). Notice that the case of pure “filtering,” i.e., when the only control is exerted through monitoring, can be reproduced by letting the CP map feed in the initial state of the bath, regardless of outcome. It is also worth mentioning that, in all derivations from discrete models, it is necessary to let the coupling strength diverge as $1/\sqrt{\Delta t}$ as $\Delta t \rightarrow 0$ (a standard assumption which is equivalent to white noise, and which will be illustrated explicitly in the CF case that follows). This does not jeopardize our argument since, for any fixed interaction Hamiltonian \hat{H}_C , the equation $e^{i\hat{H}_C dt} e^{i\hat{H}_C dt} = e^{i2\hat{H}_C dt}$ holds true in this limit too.

Let us now move on to CF, and reexamine the classic case of a mode in a cavity interacting with a finite temperature, white-noise environment through two mirrors (resulting, in the absence of feedback, in the “quantum optical master equation”), where the output of one cavity undergoes losses by a factor η and, in the absence of delays, is fed back into the other cavity mirror. Note that delays can be accommodated in our model by enlarging the bath to keep track of recurring interacting modes and by including them in the environmental CP map: they would just make our mathematical treatment cumbersome but could be handled exactly in the same way as in other formalisms (typically by moving to the frequency domain). Since this dynamics involves only linear coupling to the environment, it can be characterized entirely by the

corresponding Gaussian dynamics, which will allow for a very compact and expedient mathematical rendition and will thus be adopted (see, e.g., [77] for a full exploitation of this argument). Let $\hat{\mathbf{r}} = \begin{pmatrix} \hat{x} \\ \hat{p} \end{pmatrix}$ be the vector of the system’s canonical quadratures, such that, in outer product form, $[\hat{\mathbf{r}}, \hat{\mathbf{r}}^\top] = i\Omega$ (to be read components wise as $[\hat{r}_j, \hat{r}_k] = i\Omega_{jk}$), for the antisymmetric symplectic form $\Omega = \begin{pmatrix} 0 & 1 \\ -1 & 0 \end{pmatrix}$, and let us also define the covariance matrix $\sigma = \langle \{\hat{\mathbf{r}}, \hat{\mathbf{r}}^\top\} \rangle - \langle \hat{\mathbf{r}} \rangle \langle \hat{\mathbf{r}}^\top \rangle$, where $\langle \cdot \rangle$ stands for the expectation value on the system quantum state. The dynamical equation for the covariance matrix σ of a system subject to the CF loop described above is given by the following Lyapunov equation [31]:

$$\dot{\sigma} = -2\gamma(1 - \sqrt{\eta})\sigma + 2\gamma N(1 - \sqrt{\eta})\mathbb{1}_2, \quad (\text{A1})$$

where $\sqrt{\gamma}$ is the coupling with the white-noise environmental modes and $N = \frac{e^{\beta\hbar\omega+1}}{e^{\beta\hbar\omega}-1}$ at inverse temperature β and system mode frequency ω . Our aim is to show that such an equation can be reproduced by a CF scheme in our model.

Therefore, if $\hat{\mathbf{r}}'_{\text{in}}$ is the four-dimensional operator vector grouping together two environmental input modes, then we will choose a fixed interaction Hamiltonian \hat{H}_C such that

$$\hat{H}_C dt = \sqrt{\gamma} \hat{\mathbf{r}}^\top (\Omega^\top, \Omega^\top) \hat{\mathbf{r}}'_{\text{in}} \sqrt{dt}. \quad (\text{A2})$$

The, initially uncorrelated, global covariance matrix of system plus bath is given by the direct sum $\sigma_{gl} = \sigma \oplus N\mathbb{1}_2 \oplus N\mathbb{1}_2$ and evolves, under the quadratic Hamiltonian \hat{H}_C for an interval dt , by congruence under the corresponding symplectic transformation $e^{J_C dt}$, where

$$J_C = \sqrt{\gamma} \begin{pmatrix} 0 & \mathbb{1}_2 & \mathbb{1}_2 \\ -\mathbb{1}_2 & 0 & 0 \\ -\mathbb{1}_2 & 0 & 0 \end{pmatrix}. \quad (\text{A3})$$

At first order in dt , one gets

$$\sigma_{gl} \mapsto e^{J_C dt} \sigma_{gl} e^{J_C^\top dt} = \sigma_{gl} + \sigma_{\text{SB}} \sqrt{\gamma dt} + [(N\mathbb{1}_2 - \sigma) \oplus \tilde{\sigma}_B \oplus \tilde{\sigma}_B] \gamma dt + o(dt)$$

for some environmental covariance increment $\tilde{\sigma}_B$, which will have no bearing on what follows and will thus be disregarded, and a system bath correlation matrix

$$\tilde{\sigma}_{\text{SB}} = \begin{pmatrix} 0 & -\sigma + N\mathbb{1}_2 & -\sigma + N\mathbb{1}_2 \\ -\sigma + N\mathbb{1}_2 & 0 & 0 \\ -\sigma + N\mathbb{1}_2 & 0 & 0 \end{pmatrix}, \quad (\text{A4})$$

which will instead play a key role since it is precisely the memory of such correlations which empowers the feedback control action. The CP map acting on the bath at the intermediate step then just maintains one of the two environmental modes as the interacting one (we can safely assume that will be the first bath mode), acts on its covariance matrix by mixing it with a thermal noise bath and by rotating its optical phase, and refreshes the state of the second bath mode to the initial state with uncorrelated covariance matrix $N\mathbb{1}_2$, resulting in the following correlation matrix:

$$\sigma_{\text{SB}} = \sqrt{\eta} \begin{pmatrix} 0 & \sigma - N\mathbb{1}_2 & 0 \\ \sigma - N\mathbb{1}_2 & 0 & 0 \\ 0 & 0 & 0 \end{pmatrix} \quad (\text{A5})$$

(notice the change of sign, corresponding to a rotation of the bath mode's optical phase, which is key to canceling the noise in the next step: CF is indeed a coherent mechanism, hinging on quantum interference!). The second and last interaction then lets a diagonal term in dt contribute to the covariance matrix of the system mode (note that partial tracing in the Gaussian realm just amounts to pinching out the relevant main submatrix), so that the total iteration of the feedback loop acts on the initial system covariance matrix σ as

$$\begin{aligned} \sigma \mapsto & \sigma + (N\mathbb{1}_2 - \sigma)\gamma dt + (N\mathbb{1}_2 - \sigma)\gamma dt \\ & + \sqrt{\eta}(J_C\sigma_{SB} + \sigma_{SB}J_C^\top)\gamma dt = -2\gamma dt(1 - \sqrt{\eta})\sigma \\ & + 2N\gamma dt(1 - \sqrt{\eta}), \end{aligned} \quad (\text{A6})$$

which indeed corresponds to Eq. (A1).

General diffusive coherent feedback

Having demonstrated that our collision model captures one of the archetypal forms of quantum-optical coherent feedback in continuous time, it should now be clear that it is capable of fully capturing *any* form of Gaussian coherent feedback through input-output interfaces. Nevertheless, we will show this explicitly by reproducing all the interferometric, diffusive dynamics included in the modeling considered in [31]. To this aim, we will generalize the notation and model from the preceding section to accommodate n bosonic modes coupled to a white-noise environment through an arbitrary number of input-output interfaces [4]. The output of some fraction of these interfaces will be subject to a general Gaussian CP map (in the form of interaction, through a quadratic Hamiltonian, with an arbitrary number of auxiliary modes), before reinteracting with the system through more input-output interfaces. Since the input-output formalism can be framed as a collision model [41], it should not be surprising that our collisional model of coherent feedback fully captures this form of coherent feedback, although we would like here to dispel any possible doubt in this regard that may arise from considering pairs of repeated interactions. Therefore, we will here make explicit the connection between our collision model of coherent feedback and the conventional model of Gaussian quantum-optical coherent feedback. It should be emphasized that our collision model also covers many more general notions of coherent feedback (such as those involving discrete time steps and finite-dimensional systems), which cannot be captured using the standard Gaussian description.

The system of bosonic modes will be described using a vector $\hat{\mathbf{r}} = (\hat{x}_1, \hat{p}_1, \dots, \hat{x}_n, \hat{p}_n)^\top$, where \hat{x} and \hat{p} are the canonical operators. These obey the canonical commutation relation $[\hat{r}_j, \hat{r}_k] = i\Omega_{jk}$ where we are now using Ω to represent an antisymmetric form of an arbitrary dimension:

$$\Omega = \bigoplus_{i=1}^n \begin{pmatrix} 0 & 1 \\ -1 & 0 \end{pmatrix}. \quad (\text{A7})$$

We will use Ω to denote any square matrix of this form and let the context specify its dimension. In the Gaussian formalism, a unitary operation on the Gaussian state can be represented as a symplectic transformation on the canonical operators $\hat{\mathbf{r}} \rightarrow S\hat{\mathbf{r}}$, where S is a real matrix which preserves

the symplectic form so that $S\Omega S^\top = \Omega$. Symplectic transformations correspond physically to evolution under a quadratic Hamiltonian of the form $\hat{H} = \frac{1}{2}\hat{\mathbf{r}}^\top H\hat{\mathbf{r}}$ where H is known as the Hamiltonian matrix. It is related to the symplectic matrix through the equation $S = e^{\Omega H}$ [77].

The controller (or environment) will be denoted by a vector of white-noise modes $\hat{\mathbf{r}}_{\text{in}} = \hat{\mathbf{r}}_{\text{in},a} \oplus \hat{\mathbf{r}}_{\text{in},b}$ (note that keeping the setup general and making no assumptions about dimensions of $\hat{\mathbf{r}}_{\text{in},a}$ and $\hat{\mathbf{r}}_{\text{in},b}$). In our collision model of coherent feedback, the system and environment first interact through a unitary. We will assume that this interaction lasts for a time increment $\frac{\Delta t}{2}$ and that it is generated by the coupling Hamiltonian \hat{H}_1 so that we can write $U_1 = e^{i\hat{H}_1 \frac{\Delta t}{2}}$. This Hamiltonian will be written

$$\hat{H}_1 = 2\hat{\mathbf{r}}^\top C_a \hat{\mathbf{r}}_{\text{in},a}. \quad (\text{A8})$$

The matrix C_a is real and known as the coupling matrix and characterizes the quadratic interaction between the system and environment. Note that we have put no restrictions on the form of this interaction, other than that is quadratic and physical. Also, note that this first interaction can easily include interactions with “inaccessible” white-noise modes which, if necessary, can be included to model the noise channel \mathcal{E} . The factor of 2 is here required since the input-output formalism implicitly assumes that each interaction last for a time Δt , but here we are assuming that each interaction takes $\Delta t/2$. As is customary in collision model literature, we will assume that the strengths of the coupling Hamiltonians are inversely proportional to $\sqrt{\Delta t}$, which prevents the interaction from vanishing in the continuous limit $\Delta t \rightarrow dt$ [35,41]. This is implicit in input-output model of quantum optics since $\hat{\mathbf{r}}_{\text{in},a}$ and $\hat{\mathbf{r}}_{\text{in},b}$ do not correspond to physical quadratures (since they do not obey the canonical commutation relation). But they can be related to physical quadratures which we will label $\hat{\mathbf{r}}'_{\text{in},a}$ and $\hat{\mathbf{r}}'_{\text{in},b}$ through a factor of $\sqrt{\Delta t}$ [41,77]:

$$\hat{\mathbf{r}}_{\text{in},a} = \frac{1}{\sqrt{\Delta t}}\hat{\mathbf{r}}'_{\text{in},a}, \quad \hat{\mathbf{r}}_{\text{in},b} = \frac{1}{\sqrt{\Delta t}}\hat{\mathbf{r}}'_{\text{in},b}. \quad (\text{A9})$$

This allows us to write the coupling Hamiltonian in terms of $\hat{\mathbf{r}}_T = \hat{\mathbf{r}} \oplus \hat{\mathbf{r}}'_{\text{in},a} \oplus \hat{\mathbf{r}}'_{\text{in},b}$:

$$\hat{H}_1 = \frac{1}{2}\hat{\mathbf{r}}_T^\top H_1 \hat{\mathbf{r}}_T \quad \text{where} \quad H_1 = \frac{2}{\sqrt{\Delta t}} \begin{pmatrix} 0 & C_a & 0 \\ C_a^\top & 0 & 0 \\ 0 & 0 & 0 \end{pmatrix}. \quad (\text{A10})$$

Therefore, the first collisional interaction between the system and environment is characterized by a symplectic operation $S_1 = e^{\Omega H_1 \frac{\Delta t}{2}}$ on $\hat{\mathbf{r}}_T$. The extra factor of $\frac{1}{\sqrt{\Delta t}}$ in our definition of H_1 means that Taylor expanding to first order in Δt leads to the symplectic

$$S_1 = \begin{pmatrix} \mathbb{1} + \frac{1}{2}\Omega C_a \Omega C_a^\top \Delta t & \Omega C_a \sqrt{\Delta t} & 0 \\ \Omega C_a^\top \sqrt{\Delta t} & \mathbb{1} + \frac{1}{2}\Omega C_a^\top \Omega C_a \Delta t & 0 \\ 0 & 0 & \mathbb{1} \end{pmatrix}. \quad (\text{A11})$$

The next stage of our collision model corresponds to an in-loop unitary U , performed on the controller alone. This

unitary will be represented by a symplectic acting on $\hat{r}'_{in,a} \oplus \hat{r}'_{in,b}$. We will assume that this interaction is instantaneous and general. We will write it as

$$\begin{pmatrix} \hat{r}'_{in,a} \\ \hat{r}'_{in,b} \end{pmatrix} \rightarrow \begin{pmatrix} E & F \\ G & H \end{pmatrix} \begin{pmatrix} \hat{r}'_{in,a} \\ \hat{r}'_{in,b} \end{pmatrix} = \begin{pmatrix} E\hat{r}'_{in,a} + F\hat{r}'_{in,b} \\ G\hat{r}'_{in,a} + H\hat{r}'_{in,b} \end{pmatrix}. \quad (\text{A12})$$

When represented as a symplectic on \hat{r}_T , this can be written

$$S_l = \begin{pmatrix} \mathbb{1} & 0 & 0 \\ 0 & E & F \\ 0 & G & H \end{pmatrix}. \quad (\text{A13})$$

Finally, after the in-loop unitary has been applied, there is another collisional interaction between the system and controller. This is characterized similarly to the first. The unitary interaction $U_2 = e^{i\hat{H}_2 \frac{\Delta t}{2}}$ corresponds to a symplectic transformation $S_2 = e^{\Omega \hat{H}_2 \frac{\Delta t}{2}}$ on \hat{r}_T , characterized by a Hamiltonian

$$\hat{H}_2 = \frac{1}{2} \hat{r}_T^\top H_2 \hat{r}_T \quad \text{where} \quad H_2 = \frac{2}{\sqrt{\Delta t}} \begin{pmatrix} 0 & 0 & C_b \\ 0 & 0 & 0 \\ C_b^\top & 0 & 0 \end{pmatrix}. \quad (\text{A14})$$

Again, Taylor expanding in Δt yields the symplectic

$$S_2 = \begin{pmatrix} \mathbb{1} + \frac{1}{2} \Omega C_b \Omega C_b^\top \Delta t & \Omega C_b \sqrt{\Delta t} & 0 \\ \Omega C_b^\top \sqrt{\Delta t} & \mathbb{1} + \frac{1}{2} \Omega C_b^\top \Omega C_b \Delta t & 0 \\ 0 & 0 & \mathbb{1} \end{pmatrix}. \quad (\text{A15})$$

Thus, the total symplectic for each iteration of the feedback process will be given by the action of S_1 , followed by S_l , followed by S_2 . This is found by multiplying Eqs. (A11), (A13), and (A15) together. We will represent this as

$$S = S_2 S_l S_1 = \begin{pmatrix} S_{11} & S_{12} & S_{13} \\ S_{21} & S_{22} & S_{23} \\ S_{31} & S_{32} & S_{33} \end{pmatrix}. \quad (\text{A16})$$

Since we will trace over the environment after every iteration of the loop, we are only concerned with S_{11} , S_{12} , and S_{13} which will affect the system operators according to $\hat{r} \rightarrow S_{11} \hat{r} + S_{12} \hat{r}'_{in,a} + S_{13} \hat{r}'_{in,b}$. These submatrices are given by

$$S_{11} = \mathbb{1} + \frac{1}{2} \Omega C_b \Omega C_b^\top \Delta t + \frac{1}{2} \Omega C_a \Omega C_a^\top \Delta t + \Omega C_b E \Omega C_a^\top \Delta t, \quad (\text{A17})$$

$$S_{12} = \Omega C_a \sqrt{\Delta t} + \Omega C_b E \sqrt{\Delta t}, \quad (\text{A18})$$

$$S_{13} = \Omega C_b F \sqrt{\Delta t}, \quad (\text{A19})$$

where we have discarded higher-order terms in Δt . Applying S to $\hat{r}_T = (\hat{r}^\top, \hat{r}'_{in,a}{}^\top, \hat{r}'_{in,b}{}^\top)^\top$ and tracing out the environment yields the incremental change in the system operators after one iteration of the feedback loop (which takes, in total, a time Δt):

$$\Delta \hat{r} = \left(\frac{1}{2} \Omega C_b \Omega C_b^\top + \frac{1}{2} \Omega C_a \Omega C_a^\top + \Omega C_b E \Omega C_a^\top \right) \hat{r} \Delta t + (\Omega C_a + \Omega C_b E) \sqrt{\Delta t} \hat{r}'_{in,a} + \Omega C_b F \hat{r}'_{in,b} \sqrt{\Delta t}. \quad (\text{A20})$$

Using $\hat{r}_{in} \Delta t = \hat{r}'_{in} \sqrt{\Delta t}$ allows us to write

$$\Delta \hat{r} = \left(\frac{1}{2} \Omega C_b \Omega C_b^\top + \frac{1}{2} \Omega C_a \Omega C_a^\top + \Omega C_b E \Omega C_a^\top \right) \hat{r} \Delta t + (\Omega C_a + \Omega C_b E) \Delta t \hat{r}_{in,a} + \Omega C_b F \hat{r}_{in,b} \Delta t. \quad (\text{A21})$$

Finally, taking the continuous limit yields the stochastic equation

$$d\hat{r} = \left(\frac{1}{2} \Omega C_b \Omega C_b^\top + \frac{1}{2} \Omega C_a \Omega C_a^\top + \Omega C_b E \Omega C_a^\top \right) \hat{r} dt + (\Omega C_a + \Omega C_b E) \hat{r}_{in,a} dt + \Omega C_b F \hat{r}_{in,b} dt. \quad (\text{A22})$$

For a generic quadratic system-environment interaction, the evolution of the system operators is governed by a quantum Langevin equation which takes the form [77]

$$\dot{\hat{r}} = (\Omega H + \frac{1}{2} \Omega C \Omega C^\top) \hat{r} + \Omega C \hat{r}_{in}, \quad (\text{A23})$$

where C is the coupling matrix between \hat{r} and $\hat{r}_{in} = (\hat{r}'_{in,a}, \hat{r}'_{in,b})^\top$ and H is the system Hamiltonian matrix.

Note that we can write Eq. (A22) in this form, provided that the coupling and system Hamiltonian matrices take the form

$$C = (C_a + C_b E, C_b F), \quad H = \frac{1}{2} (C_b E \Omega C_a^\top + C_a \Omega^\top E^\top C_b^\top). \quad (\text{A24})$$

Thus, when our collisional model of coherent feedback is applied in the continuous limit in the regime of Gaussian quantum optics, the evolution of the system is fully characterized by a standard Langevin equation of the form (A23) with coupling and Hamiltonian matrices given by (A24). This is the same result as that given in [31] (up to an implicit phase shift which replaces E with $-E$), which was derived in a different manner. Thus, our collisional model captures fully the previously established general model of Gaussian coherent feedback.

APPENDIX B: DETAILED RESULTS AND PROOFS ON FEEDBACK COOLING

1. Coherent feedback cooling with noisy controller

We prove here that for ‘‘noisy’’ controllers initialized in the maximally mixed state, coherent feedback cannot provide any advantage. All of our examples use the model introduced in the paper. In this model, the system and controller are both d -dimensional qudits which interact twice through a partial swap unitary. Inside the coherent feedback loop, we have no ancillary systems, and the only allowed in-loop operations are single-qudit unitaries. Throughout these notes, the subscript T will indicate the total two-qudit, system-controller joint state and the subscript S will refer to the system alone. Our setup for cooling with coherent feedback at high temperature unfolds as follows:

(1) The controller is initialized to the maximally mixed state $\eta^{\text{in}} = \frac{1}{d} \mathbb{1}$. The system input ρ_S^{in} is the result of the previous iteration of the process.

(2) The system is subject to noise in the form of a depolarizing channel.

(3) The system and controller interact through a partial swap unitary.

(4) A unitary U is applied to the controller.

(5) The system and controller interact again through a partial swap unitary.

The von Neumann entropy of the total input state $\rho_S^{\text{in}} \otimes \eta$ is given by

$$S_T^{\text{in}} = S(\rho_S^{\text{in}} \otimes \eta) = S(\rho_S^{\text{in}}) + S(\eta^{\text{in}}). \quad (\text{B1})$$

After the application of the noise, the system is still in a separable state and the total entropy is

$$S_T = S[\mathcal{E}(\rho_S^{\text{in}})] + S(\eta^{\text{in}}). \quad (\text{B2})$$

Since the rest of the protocol can be described by unitary operations, the global entropy is left unchanged so

$$S_T^{\text{out}} = S_T = S[\mathcal{E}(\rho_S^{\text{in}})] + S(\eta^{\text{in}}). \quad (\text{B3})$$

Using the subadditivity of entropy, we can obtain the following bound on the entropy of the system output state:

$$S(\rho_S^{\text{out}}) \geq S_T^{\text{out}} - S(\eta^{\text{out}}) = S[\mathcal{E}(\rho_S^{\text{in}})] - \Delta S(\eta), \quad (\text{B4})$$

where $\Delta S(\eta) = S(\eta^{\text{out}}) - S(\eta^{\text{in}})$ is the change in entropy of the controller. Since η^{in} is maximally mixed, the maximum value of $\Delta S(\eta^{\text{in}})$ is 0. This gives us the bound on the entropy of the output:

$$S(\rho_S^{\text{out}}) \geq S[\mathcal{E}(\rho_S^{\text{in}})] \geq S(\rho_S^{\text{in}}). \quad (\text{B5})$$

The entropy of the system output state can never be lower than the entropy of the input. Furthermore, the input and output entropies are only equal when $S[\mathcal{E}(\rho_S^{\text{in}})] = S(\rho_S^{\text{in}})$ which is only true when ρ_S^{in} is maximally mixed, meaning that the only steady state is the maximally mixed state.

2. Measurement-based feedback for cooling with a noisy controller

In this section we consider measurement-based feedback cooling for a two-qudit setup with an initially maximally mixed environment/controller $\eta = \frac{1}{d}\mathbb{1}$. The system undergoes a depolarizing map, before system and controller interact through a first partial swap. The controller is then measured in the basis $\{|j\rangle\}$ and a unitary V_j is applied to the controller, depending on the measurement outcome. The system and controller then interact again through a partial swap, and the controller is traced over. Throughout the Appendixes, we use the convention that the partial swap is written $U_s = \sqrt{\tau}\mathbb{1} - i\sqrt{1-\tau}\hat{S}$.

a. Unconditional MF

We will now derive the steady state for the case of measurement-based feedback averaged over all trajectories. This means that the in-loop measurement and feedback can be represented as a CP map with elements $\{V_j |j\rangle \langle j|\}$. In particular, we will find the steady state for the case where, through the action of V_j , all measurement outcomes are mapped to the same state, which we will label $|0\rangle$. This corresponds to a CP map with elements $\{|0\rangle \langle j|\}$. In the next section we will show that this is optimal when one filters and conditions the state on the measurement outcome. We will first derive expressions for the most general projective MF protocol, and then restrict to the optimal case. Throughout, we will denote the action of the initial depolarizing map as $\rho_N = \mathcal{E}(\rho_{\text{in}}) = \lambda\rho_{\text{in}} + \frac{1-\lambda}{d}\mathbb{1}$.

Notice that ρ_N has the same eigenvectors as ρ_{in} as well as the same ordering (i.e., the eigenvector corresponding to the largest eigenvalue of ρ_{in} also corresponds to the largest eigenvalue of ρ_N).

After the action of the depolarizing map and the first partial swap, the system and controller are correlated in the following state:

$$\rho_T = \tau\rho_N \otimes \eta + (1-\tau)\eta \otimes \rho_N - i\sqrt{\tau}\sqrt{1-\tau}[S, \rho_N \otimes \eta], \quad (\text{B6})$$

where S is the swap unitary. After the measurement, and application of the unitaries $\{V_j\}$, the global state is

$$\rho_T = \sum_j p_j \rho_j \otimes |\psi_j\rangle \langle \psi_j|, \quad (\text{B7})$$

where $|\psi_j\rangle = V_j |j\rangle$ and p_j are the probabilities of each outcome. The (unnormalized) system state for each measurement outcome is given by

$$p_j \rho_j = \frac{1}{d}\tau\rho_N + (1-\tau)\eta(\rho_N)_{jj} - i\sqrt{\tau}\sqrt{1-\tau}[|j\rangle \langle j|, \rho_N], \quad (\text{B8})$$

where $(\rho_N)_{jj} = \langle j | \rho_N | j \rangle$. We have also used the fact that $\text{Tr}_C[S, A \otimes B] = [B, A]$. After a final interaction through a partial swap, the controller is traced out, leaving the output state:

$$\rho_{\text{out}} = \sum_i p_i (\tau\rho_i + (1-\tau)|\psi_i\rangle \langle \psi_i| - i\sqrt{\tau}\sqrt{1-\tau}[|\psi_i\rangle \langle \psi_i|, \rho_i]). \quad (\text{B9})$$

The optimal protocol, in which all measurement results are mapped to the $|0\rangle$ state through the unitaries V_j , amounts to setting $|\psi_j\rangle = V_j |j\rangle = |0\rangle$ for all j . Using $\sum_j p_j \rho_j = \tau\rho_N + (1-\tau)\eta$, we find the output state:

$$\rho_{\text{out}} = \tau^2\rho_N + \tau(1-\tau)\eta + (1-\tau)|0\rangle \langle 0| - i\tau^{\frac{3}{2}}\sqrt{1-\tau}[|0\rangle \langle 0|, \rho_N]. \quad (\text{B10})$$

The fact that $\eta = \frac{1}{d}\mathbb{1}$ allows us to write $\rho_N = \lambda\rho_{\text{in}} + (1-\lambda)\eta$. We now assume a steady state, which involves setting $\rho_{\text{in}} = \rho_{\text{out}} = \rho_{\text{ss}}$. Rearranging for ρ_{ss} gives

$$\rho_{\text{ss}} = \frac{1}{1-\tau^2\lambda}([\tau^2(1-\lambda) + \tau(1-\tau)]\eta + (1-\tau)|0\rangle \langle 0| - \lambda i\tau^{\frac{3}{2}}\sqrt{1-\tau}[|0\rangle \langle 0|, \rho_{\text{ss}}]). \quad (\text{B11})$$

The only solution to this equation is one where ρ_{ss} is diagonal in a basis $\{|j\rangle\}$ which contains $|0\rangle$. To see this, we can act on the above equation with $\langle j|$ and $|k\rangle$ from the left and right (for $j \neq k$) and obtain

$$\langle j | \rho_{\text{ss}} | k \rangle = \frac{1}{1-\tau^2\lambda} - \lambda i\tau^{\frac{3}{2}}\sqrt{1-\tau}(\delta_{j0} \langle 0 | \rho_{\text{ss}} | k \rangle - \langle j | \rho_{\text{ss}} | 0 \rangle \delta_{0k}). \quad (\text{B12})$$

Note that the right-hand side of this equation is only nonzero when either j or k is equal to zero. For $j = 0, k \neq 0$, we obtain

$$\langle 0 | \rho_{\text{ss}} | k \rangle = \frac{1}{1-\tau^2\lambda} - \lambda i\tau^{\frac{3}{2}}\sqrt{1-\tau}(\langle 0 | \rho_{\text{ss}} | k \rangle). \quad (\text{B13})$$

The only solution to this equation is when $\langle 0 | \rho_{ss} | k \rangle = 0$. Therefore, ρ_{ss} is diagonal in the basis $\{|j\rangle\}$. This means that the eigenvalues of ρ_{ss} are given by $\langle j | \rho_{ss} | j \rangle$. The eigenvalue associated with $|0\rangle$ is

$$\alpha_0 = \frac{1}{1 - \tau^2 \lambda} \left(\frac{\tau^2(1 - \lambda) + \tau(1 - \tau)}{d} + (1 - \tau) \right). \quad (\text{B14})$$

The remaining $d - 1$ eigenvalues are degenerate, each with value

$$\alpha_j = \frac{1}{1 - \tau^2 \lambda} \left(\frac{\tau^2(1 - \lambda) + \tau(1 - \tau)}{d} \right). \quad (\text{B15})$$

Thus, the steady state under this protocol takes the form

$$\rho_S = \frac{1}{d} \frac{d(1 - \tau) + \tau - \lambda \tau^2}{1 - \lambda \tau^2} |0\rangle \langle 0| + \sum_{j=1}^{d-1} \frac{1}{d} \frac{\tau - \lambda \tau^2}{1 - \lambda \tau^2} |j\rangle \langle j|. \quad (\text{B16})$$

The linear entropy for this steady state is

$$S_L = 1 - \sum_j \alpha_j^2 = \left(1 - \frac{1}{d}\right) - \frac{(\tau - 1)^2(d - 1)}{d(\tau^2 \lambda - 1)^2}. \quad (\text{B17})$$

We note that, for states like these with one large eigenvalue and $d - 1$ degenerate eigenvalues, both von Neumann and linear entropies are solely functions of the largest eigenvalue and are thus equivalent for the purposes of comparison. This is always the case for qubits, where the linear entropy and von Neumann entropy are equivalent. Because of this, and in view of their more compact expressions, we will use the linear entropy for the remainder of this investigation (though we will give expressions for the eigenvalues of each state, from which the von Neumann entropy can easily be calculated).

b. Conditional MF

In this section, we will consider filtered measurement feedback, meaning that the measurement result is recorded and the system's conditional state evolves stochastically. After the measurement is performed along with the in-loop unitary operation, the system and controller are in the joint state $\rho_j \otimes |\psi_j\rangle \langle \psi_j|$ for a measurement result labeled by j (where ρ_j and $|\psi_j\rangle$ are defined as in the previous section). This is as opposed to averaged MF, where the system and controller are in the mixture of states given by (B7). After the second partial swap and tracing out of the controller, the system output will be

$$\rho_{\text{out},j} = \text{Tr}_C[U_S \rho_j \otimes |\psi_j\rangle \langle \psi_j| U_S^\dagger]. \quad (\text{B18})$$

We will now show that, for a ρ_{in} which is initially diagonal in the measurement basis (as would be the case for the maximally mixed state, which represents the uncontrolled steady state of the system, as well as for the unconditional steady states determined in the previous section), the entropy of this output is minimized when $|\psi_j\rangle$ is set to be the dominant eigenvector of ρ_{in} (i.e., the eigenvector associated to its largest eigenvalue), regardless of the measurement result. Notice also that the choice of basis for the ‘‘atomic’’ projective measurement (i.e., a measurement that resolves each individual basis state) is irrelevant, given the unitary invariance of the problem (here, we are disregarding more general POVMs or adaptive

measurements, which may become the subject of further inquiry in the future). If ρ_{in} is diagonal in the measurement basis, the commutator in Eq. (B8) is equal to zero and we can write

$$\rho_j = \frac{1}{p_j} \left(\frac{1}{d} \tau \rho_N + (1 - \tau) \eta(\rho_N)_{jj} \right). \quad (\text{B19})$$

Note that each ρ_j has the same set of eigenvectors in the same ordering as ρ_{in} , so the eigenvector corresponding to the largest eigenvalue is the same for both ρ_{in} and ρ_j .

We now make use of the entropy power inequality for the output of a partial swap gate derived in [68], in the form of the following Majorization relation:

$$\lambda(\rho_{\text{out},j}) \prec \tau \lambda(\rho_j) + (1 - \tau) \lambda(|\psi_j\rangle \langle \psi_j|), \quad (\text{B20})$$

where we have used $\lambda(\rho)$ to indicate the spectrum of ρ , ordered from the largest eigenvalue to the smallest. The right- and left-hand sides of this relation are equal when $|\psi_j\rangle$ is pointing along the direction of the dominant eigenvector of ρ_j , which in turn is the dominant eigenvector of ρ_{in} . Thus, to minimize the conditional output entropy for an input diagonal in the measurement basis, we must set all $|\psi_j\rangle$ equal to the eigenvector corresponding to the largest eigenvalue of ρ_{in} .

Let us now also briefly consider some quantitative examples of the conditional stochastic evolution occurring under this filtered, measurement-based feedback. This provides insight into the dependence of the optimal cooling process on the various system parameters. Let us remind that the latter are the depolarizing strength λ (from complete depolarization for $\lambda = 0$ to the identity channel for $\lambda = 1$), the partial swap angles parametrized by $\sqrt{\tau}$ and the system dimension d . Figure 2 shows the evolution of the von Neumann entropy (with base d logs, such that 1 is always maximum entropy for all dimensions) for various choices of parameters, always starting from the maximally mixed state (which corresponds to the uncontrolled steady state). The *unconditional* (‘‘unfiltered’’) steady-state entropies are also reported for comparison and, as may be seen, always fall within the range of two possible, typical unconditional values, deviating relatively little from them, such that the stabilized, unfiltered strategy proves to be very effective in these instances. Indeed, in all of these case studies, regardless of the Hilbert space dimension, only one of the system eigenvalues is different from the other, accruing probability at the expense of the other eigenvalues, which remain equal (therefore, any POVM capable of resolving the dominant eigenvector would also be optimal). When the dominant eigenvector is detected on the controller branch of the feedback loop, its proportion in the system branch decreases, and therefore the measurement is disadvantageous in terms of cooling the system. At each run of the feedback loop, this occurs with probability

$$p_0 = \frac{\tau}{d} + (1 - \tau) \alpha_\lambda, \quad (\text{B21})$$

where $\alpha_\lambda = \lambda \alpha_{\text{in}} + \frac{(1-\lambda)}{d}$ and α_{in} is the dominant eigenvalue of the input state. For completeness, let us also report the values of the largest output eigenvector upon measurement of the dominant eigenvector in the feedback loop ($\alpha_{0,0}$) upon

measurement of another outcome ($\alpha_{0,1}$), to be contrasted with the average, unconditional α_0 of Eq. (B14):

$$\alpha_{0,0} = \frac{\tau\alpha_\lambda}{p_0d} + (1 - \tau), \quad (\text{B22})$$

$$\alpha_{0,1} = \frac{\tau}{(1 - p_0)d} [\tau d\alpha_\lambda - \alpha_\lambda + (1 - \tau)] + (1 - \tau). \quad (\text{B23})$$

All of these three functions are monotonically increasing in λ and decreasing in τ . Therefore, as one should expect, the asymptotic cooling performance will be more effective for higher λ , corresponding to less noise, and lower τ , corresponding to a larger connectivity between system and controller, which allows one to swap a substantial part of the final state with a low-entropy one. Hence, as shown in Fig. 2, higher connectivities can offset larger noise parameters. Observe also that higher dimensions, typically, make for larger spread in the normalized entropy around the unconditional value. Further, it is worthwhile noticing that the model also allows one to observe that cooling will be achieved in a number of steps of the order of $1/(1 - \tau)$: the transmissivity between

controller and system is the parameter that determines the model's cooling rate.

3. Coherent feedback for cooling with a clean controller

We will consider a setup identical to the previous section, except that the environment is initialized to a pure state $|0\rangle \langle 0|$. We will restrict to qubits and find the lowest-entropy steady state achievable through CF which is diagonal in the $\{|0\rangle, |1\rangle\}$ basis. We express the in-loop unitary as using the general decomposition:

$$U = \begin{pmatrix} e^{i\varphi_1} \cos \chi & e^{i\varphi_2} \sin \chi \\ -e^{-i\varphi_2} \sin \chi & e^{-i\varphi_1} \cos \chi \end{pmatrix}. \quad (\text{B24})$$

The steady state which satisfies the condition that it is diagonal in the basis containing $|0\rangle$ takes the form

$$\rho_{\text{ss}} = \text{diag}(e_1, 1 - e_1) \quad (\text{B25})$$

with

$$e_1 = \frac{-2\tau^2(\lambda + 1)p^2(q + 1) + 2\tau\{p^2[\lambda(q + 2) + q + 1] - \lambda\} + \lambda - 2\lambda p^2 + 1}{\lambda(4\tau\{p^2[(\tau - 1)q + \tau - 2] + 1\} + 4p^2 - 2) - 2}, \quad (\text{B26})$$

where $p = \cos \chi$ and $q = \cos 2\varphi_1$. The linear entropy for this state is minimized when χ and φ_1 are both integer multiples of π , which is satisfied when the in-loop unitary U is equal to the identity. In this case the steady state has linear entropy:

$$S_{\text{CF}} = \frac{1}{2} - \frac{8\tau^2(\tau - 1)^2}{((1 - 2\tau)^2\lambda - 1)^2}. \quad (\text{B27})$$

If this CF protocol (“do nothing” in the loop) is applied to a setup with a system and environment of dimension d , the steady state will have its largest eigenvalue (with eigenvector $|0\rangle$) equal to

$$\beta_0 = \frac{4(\tau - 1)\tau(d + \lambda - 1) + \lambda - 1}{d((1 - 2\tau)^2\lambda - 1)}. \quad (\text{B28})$$

The other $(d - 1)$ eigenvalues are

$$\beta_j = \frac{(1 - 2\tau)^2(\lambda - 1)}{d((1 - 2\tau)^2\lambda - 1)}. \quad (\text{B29})$$

For dimension d , this steady state will have linear entropy:

$$S_L = \left(1 - \frac{1}{d}\right) - \frac{16\tau^2(\tau - 1)^2(d - 1)}{d((1 - 2\tau)^2\lambda - 1)^2}, \quad (\text{B30})$$

which is always less than the linear entropy of the maximally mixed state. Note that when $\tau = \frac{1}{2}$, $\beta_0 = 1$ and $\beta_{j \neq 0} = 0$ and the steady state is pure. This is because, when $\tau = \frac{1}{2}$, the partial swap is the square root of the full swap, so applying it twice enacts a full swap, replacing the system mode with the pure environmental mode.

4. Measurement-based feedback for cooling with a clean controller

We will now look at the effect of our averaged MF protocol when the environment is not maximally mixed. We will consider a qubit system with a generic environmental input state η which will have an arbitrary temperature and apply the same MF protocol as in the high-temperature case. After one iteration of our MF protocol, the output state is

$$\rho_{\text{out}} = \tau^2 \rho_N + \tau(1 - \tau)\eta + (1 - \tau)|0\rangle \langle 0| - i\tau^{\frac{3}{2}}\sqrt{1 - \tau}[|0\rangle \langle 0|, \rho_N]. \quad (\text{B31})$$

Previously, we assumed that η was maximally mixed, but it need not be. We will restrict to qubits and choose $|0\rangle$ to point along the direction of the dominant eigenvector of η , so we can write $\eta = \eta_0|0\rangle \langle 0| + (1 - \eta_0)|1\rangle \langle 1|$. Solving for steady state gives

$$\rho_{\text{ss}} = \frac{1}{1 - \tau^2\lambda} \left(\tau^2(1 - \lambda)\frac{1}{d}\mathbb{1} + [\tau(1 - \tau)\eta_0 + (1 - \tau)]|0\rangle \langle 0| + \tau(1 - \tau)(1 - \eta_0)|1\rangle \langle 1| \right) \quad (\text{B32})$$

$$- i\lambda\tau^{\frac{3}{2}}\sqrt{1 - \tau}[|0\rangle \langle 0|, \rho_{\text{ss}}]. \quad (\text{B33})$$

As before, this state is diagonal in the basis $\{|j\rangle\}$. It has eigenvalues

$$\alpha_0 = \frac{1}{1 - \tau^2\lambda} \left(\tau^2(1 - \lambda)\frac{1}{2} + \tau(1 - \tau)\eta_0 + (1 - \tau) \right), \quad (\text{B34})$$

$$\alpha_1 = \frac{1}{1 - \tau^2\lambda} \left(\tau^2(1 - \lambda)\frac{1}{2} + \tau(1 - \tau)(1 - \eta_0) \right). \quad (\text{B35})$$

The linear entropy of this state is

$$S_{\text{MF}} = \frac{1}{2} - \frac{(\tau - 1)^2 [\tau(2\eta_0 - 1) + 1]^2}{2(\tau^2\lambda - 1)^2}. \quad (\text{B36})$$

A maximally mixed environment corresponds to $\eta_0 = \frac{1}{2}$, which recovers the expression from earlier. For a pure environment, we set $\eta_0 = 1$ and we obtain the following expression:

$$S_{\text{MF}} = \frac{1}{2} - \frac{(\tau^2 - 1)^2}{2(\tau^2\lambda - 1)^2}. \quad (\text{B37})$$

We can compare this with the performance of CF in the same setup, as quantified by Eq. (B27). Comparing Eq. (B37) with (B27), we find that $S_{\text{MF}} < S_{\text{CF}}$ for $\tau < \frac{1}{3}$ and $S_{\text{MF}} > S_{\text{CF}}$ for $\tau > \frac{1}{3}$.

We will now prove that, even with a pure environment, no MF protocol can prepare a pure steady state when $\tau = \frac{1}{2}$. Recall that, for $\tau = \frac{1}{2}$ and a pure environment CF produces a pure steady state, so this is an interesting point of comparison. Again, we will restrict our investigation to qubits. As we have seen before, after projective measurement and the action of a unitary, the system and controller are in a joint state:

$$\rho_T = \sum_j p_j \rho_j \otimes |\psi_j\rangle \langle \psi_j|, \quad (\text{B38})$$

where

$$\rho_j = \frac{1}{p_j} \left(\frac{1}{2} \tau \rho_N + (1 - \tau) \eta(\rho_N)_{jj} - i\sqrt{\tau} \sqrt{1 - \tau} [|j\rangle \langle j|, \rho_N] \right). \quad (\text{B39})$$

First, we will show that ρ_j cannot be pure. We do this by writing ρ_j in the basis containing $|j\rangle$ and restrict to the case of interest, when $\tau = \frac{1}{2}$. This gives us

$$\rho_S^{(1)} = \frac{1}{2} \begin{pmatrix} 1 + \rho_{00} & \rho_{01}(1 + i) \\ \rho_{10}(1 - i) & 1 - \rho_{00} \end{pmatrix}, \quad (\text{B40})$$

where ρ_{ij} are the matrix elements of ρ_N . This matrix has eigenvalues

$$\lambda_{+/-} = \frac{1}{2} (1 \pm \sqrt{\rho_{00}^2 + 2\rho_{01}\rho_{10}}) \geq 0. \quad (\text{B41})$$

If this state is pure, then one of its eigenvalues will be equal to 0, and the other equal to 1. This requires $\sqrt{\rho_{00}^2 + 2\rho_{01}\rho_{10}} = 1$. Since both eigenvalues must be greater than or equal zero, $\rho_{00}^2 + 2\rho_{01}\rho_{10} \leq 1$. The equality is reached only in the case where $\rho_{00} = 1$, which could only be the case if ρ_N was pure. However, ρ_N cannot be pure since it has been subject to the depolarizing map. Even if ρ_{in} was pure, ρ_N would not be pure for any non-negligible value of the noise parameter λ . Thus, we can conclude that the ρ_j 's are not pure.

After the second system-controller interaction, the controller is traced out and the output state is given by

$$\rho_{\text{out}} = \sum_i p_i (\tau \rho_i + (1 - \tau) |\psi_i\rangle \langle \psi_i| - i\sqrt{\tau} \sqrt{1 - \tau} |\psi_i\rangle \langle \psi_i|, \rho_i) = \sum_i p_i \sigma_i. \quad (\text{B42})$$

By applying the same argument that we used to prove that ρ_j could not be pure, we can prove that σ_j also cannot be pure. Thus, since ρ_{out} is a mixture of mixed states, it cannot be pure. This means that no averaged MF protocol can achieve a pure steady state for a partial swap interaction when the coupling is characterized by $\tau = \frac{1}{2}$.

5. Cooling comparison at intermediate noise

We will now apply our CF protocol from earlier, where the in-loop unitary is the identity, to a setup with a nonzero temperature environment with state $\eta = \eta_0 |0\rangle \langle 0| + (1 - \eta_0) |1\rangle \langle 1|$. This leads to a steady state which is diagonal in the $\{|0\rangle, |1\rangle\}$ basis with the following eigenvalue corresponding to the $|0\rangle$ eigenvector:

$$\beta_0 = \frac{4(\tau - 1)\tau(2\eta_0 + \lambda - 1) + \lambda - 1}{2(1 - 2\tau)^2\lambda - 2}. \quad (\text{B43})$$

This steady state has a linear entropy

$$S_{\text{CF}} = \frac{1}{2} - \frac{8\tau^2(\tau - 1)^2(1 - 2\eta_0)^2}{((1 - 2\tau)^2\lambda - 1)^2}. \quad (\text{B44})$$

We will now compare the performance MF and CF for intermediate environmental temperatures by comparing Eqs. (B36) and (B44). Equation (B36) gives the steady-state system entropy when the MF protocol involves measuring the ancilla and, regardless of the outcome, preparing it in the same state before the system and environment interact for the second time. This equation assumed that, after measurement, the controller is prepared in the state $|0\rangle \langle 0|$. Note that the protocol allows for some flexibility as the controller could be prepared in any state after measurement. It is optimal to use MF to prepare the controller in the state corresponding to the largest eigenvalue of the environmental input. For $\eta_0 < \frac{1}{2}$, this corresponds to $|0\rangle \langle 0|$ and for $\eta_0 > \frac{1}{2}$, this corresponds to $|1\rangle \langle 1|$. For our comparison, we assume that the optimal MF protocol is used. The steady-state entropy for these protocols, along with steady-state CF entropy given by Eq. (B44), is plotted in Fig. 5 for different environmental states, as parametrized by η_0 . We find that for the setup with $\sqrt{\tau} = 0.5$, MF outperforms CF for all environmental temperatures. For a weaker system-environment interaction, characterized by $\sqrt{\tau} = 0.9$ and noise parameter $\lambda = 0.5$, we find that MF outperforms CF for high-temperature environments with $0.357 < \eta_0 < 0.764$, but CF outperforms MF at low temperatures characterized by $\eta_0 < 0.357$ and $\eta_0 > 0.764$. Broadly, we can make the following observations: For low-temperature environments and weak couplings, the act of measurement disturbs the coherent process which allows for low-entropy environmental states to be transferred to the system, meaning that MF is inferior to CF. However, with strong couplings and noisy environments, the purification from the act of measurement compensates for this and leads MF to be superior to CF.

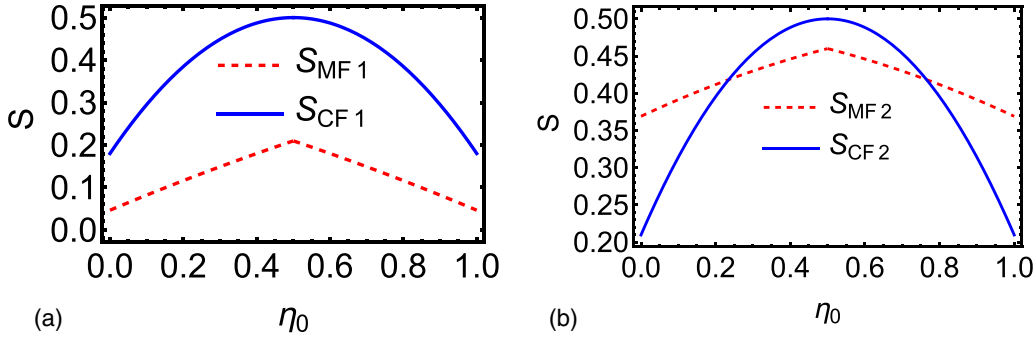


FIG. 5. (a) Shows the steady-state entropy against the largest eigenvalue of the environmental state for MF and CF setups, as given by Eqs. (B36) and (B44) where $\sqrt{\tau} = 0.5$ and $\lambda = 0.25$. (b) Shows the same expressions for setups where $\sqrt{\tau} = 0.9$ and $\lambda = 0.5$.

APPENDIX C: PROTECTION OF AN EXCITED STATE FROM AMPLITUDE DAMPING

1. Coherent feedback for protecting an excited state from amplitude damping

We will now investigate the ability of CF to protect a qubit from amplitude damping. The qubit will be subject to amplitude damping channel, after which the CF loop will be applied. We will assume that the highest-energy state is the $|1\rangle$ state, so that amplitude damping channel is given by Kraus operators

$$E_0 = \sqrt{\gamma} |0\rangle \langle 1|, \quad E_1 = \sqrt{1-\gamma} |1\rangle \langle 1| + |0\rangle \langle 0|. \quad (\text{C1})$$

This channel will be applied to the system before the CF loop is applied to attempt to counter it. Using our model again, the two system-controller interactions will be partial swaps. We will restrict the in-loop unitaries to rotations of the form

$$U = \begin{pmatrix} \cos \chi & \sin \chi \\ -\sin \chi & \cos \chi \end{pmatrix}. \quad (\text{C2})$$

We will assume that the controller is “noisy” and initialized in the maximally mixed state. Our figure of merit will be the steady-state occupation of the $|1\rangle$ state. We did not perform an analytical optimization in this case, but rather investigated the problem, and found that the optimal CF protocol depends on the partial swap strength, characterized by τ . For $\tau < \frac{1}{2}$, the optimal protocol involves setting $\chi = \frac{\pi}{2}$ and for $\tau > \frac{1}{2}$, the optimal protocol involves setting $\chi = 0$. Plots of the steady-state occupation of the $|1\rangle$ state, against χ , for different values of the τ , are plotted in Fig. 3 of the main text.

From Fig. 3(a), showing the performance of the setup with weak damping characterized by $\gamma = 0.2$, and Fig. 3(b), showing the performance of the same setup with stronger damping, characterized by $\gamma = 0.8$, one observes that, for weak system-controller interactions (where $\tau > \frac{1}{2}$), increasing the damping noise strength decreases the steady-state occupation of the excited state, as expected. However, for strong system-controller interactions (where $\tau < \frac{1}{2}$), the optimal performance (when $\chi = \frac{\pi}{2}$) is actually *improved* by stronger damping. This is because the action of the in-loop $\frac{\pi}{2}$ rotation is more effective at populating the $|1\rangle$ state when more of the state is initially prepared in the $|0\rangle$ state. In this sense, CF allows for the purifying effect of the amplitude damping map to be harnessed for the purpose of increasing the excited-state population. When $\chi = 0$ and the in-loop unitary is the identity, the steady-state

occupation of the $|1\rangle$ state is

$$\rho_{11}^{\chi=0} = \frac{2\tau(1-\tau)}{4(\tau-1)(\gamma-1)\tau + \gamma}, \quad (\text{C3})$$

which is a decreasing function of γ for $\tau > \frac{1}{2}$. Conversely, when $\chi = \frac{\pi}{2}$, the steady-state occupation of the $|1\rangle$ state is

$$\rho_{11}^{\chi=\frac{\pi}{2}} = \frac{1-\tau}{2(\gamma-1)\tau - \gamma + 2}, \quad (\text{C4})$$

which is an increasing function of γ for $\tau < \frac{1}{2}$.

2. Measurement-based feedback for protecting an excited state from amplitude damping

We will compare this to an intuitive MF protocol which measures the controller in the $\{|1\rangle, |0\rangle\}$ basis, does nothing if the result is $|1\rangle$, and applies an in-loop rotation with $\chi = \frac{\pi}{2}$ if the result is $|0\rangle$, resulting in a controller which is always prepared in the $|1\rangle$ state postmeasurement. This protocol results in a steady-state occupation of the $|1\rangle$ state:

$$\rho_{11}^{\text{MF}} = \frac{2 - \tau^2 - \tau}{2(\gamma-1)\tau^2 + 2}. \quad (\text{C5})$$

This expression is greater than Eq. (C4) for all values of τ and γ , so we can say that MF outperforms CF in the regime of $\tau < \frac{1}{2}$. However, for some setups with $\tau > \frac{1}{2}$, Eq. (C5) is slightly lower than (C3). In particular, (C3) is greater than (C5) when

$$\sqrt{\tau} > \frac{1}{2} \sqrt{\frac{-7\gamma + \sqrt{\gamma(17\gamma - 24)} + 16 + 4}{2 - 2\gamma}}. \quad (\text{C6})$$

In this regime, CF will outperform MF, though numerical investigations suggest that the advantage is small. Conversely, in the regime where MF outperforms CF, the advantage tends to be larger. Figure 4 in the main text shows the occupation ρ_{11} of the $|1\rangle$ state, against N , the number of iterations of the feedback loop. Both MF and CF protocols described above are presented. In one setup, MF outperforms yields a higher steady-state occupation of the the excited state, and in the other, CF achieves a higher steady-state occupation. The unconditional (averaged) MF trajectory is shown, as well as 50 conditional trajectories for each setup.

APPENDIX D: DETAILED RESULTS AND PROOFS ON FEEDBACK-ASSISTED BIT FLIP

1. Coherent feedback assisted bit flip

The input for the system will be a pure state given by

$$|\psi\rangle = \cos\frac{\chi}{2}|0\rangle + e^{i\phi}\sin\frac{\chi}{2}|1\rangle. \quad (\text{D1})$$

$$\rho_{\text{out}} = \frac{1}{2} \begin{pmatrix} (2\tau - 1)\cos(\chi) + 1 & e^{-i\phi}\sin(\chi)[\tau + (1 - \tau)e^{2i\phi}] \\ e^{-i\phi}\sin(\chi)[(1 - \tau) + \tau e^{2i\phi}] & (1 - 2\tau)\cos(\chi) + 1 \end{pmatrix}. \quad (\text{D2})$$

The desired final output state is $\rho_X = |\psi_X\rangle\langle\psi_X|$ where

$$|\psi_X\rangle = \sigma_x |\psi\rangle = \cos\frac{\chi}{2}|1\rangle + e^{i\phi}\sin\frac{\chi}{2}|0\rangle. \quad (\text{D3})$$

The fidelity of the output state to the desired state is a function of χ and ϕ and is given by

$$F_{\text{CF}}(\chi, \phi) = \langle\psi_X|\rho_S^{\text{out}}|\psi_X\rangle = \frac{1}{4}\{\tau[\cos(2\phi) - 2\cos(2\chi)\cos^2(\phi)] - 3\tau + 4\}. \quad (\text{D4})$$

As our figure of merit, we take this output fidelity, averaged over the Haar measure for the input states, given by

$$A_{\text{CF}} = \frac{1}{4\pi} \int F_{\text{CF}}(\chi, \phi) \sin(\chi) d\chi d\phi = 1 - \frac{2}{3}\tau, \quad (\text{D5})$$

where χ is integrated from 0 to π and ϕ is integrated from 0 to 2π .

2. Measurement-based feedback for performing a bit flip

a. Projective measurements

Our general projective MF protocol is as follows. The system is initialized in the pure state $|\psi\rangle$ given above, and the controller initialized in the state $\eta = \eta_0|0\rangle\langle 0| + (1 - \eta_0)|1\rangle\langle 1|$. They interact through U_s . Then, a measurement is made on the controller. If the result is $|0\rangle$, the unitary U is applied to the controller and if the result is $|1\rangle$, a unitary V is applied instead. This process is equivalent to the POVM with elements $\{U|0\rangle\langle 0|, V|1\rangle\langle 1|\}$ being applied to the controller. After this, the system and controller interact again through U_s . The output system state $\rho_{S,\text{MF}}^{\text{out}}$ is too lengthy to print here, as is the fidelity $F_{\text{MF}} = \langle\psi_X|\rho_{S,\text{MF}}^{\text{out}}|\psi_X\rangle$. However, after the Haar measure average is taken, we obtain the more reasonable expression

$$\begin{aligned} A_{\text{MF}} &= \frac{1}{4\pi} \int F_{\text{MF}}(\chi, \phi) \sin(\chi) d\chi d\phi \\ &= \frac{1}{12}[6 - 2\tau^2 - (1 - \tau)^2 \cos 2\theta_u - (1 - \tau)^2 \cos 2\theta_v], \end{aligned} \quad (\text{D6})$$

where we have used the decomposition of 2×2 unitary matrices to write magnitudes of the matrix elements u_{jk} and v_{jk} as

$$\begin{aligned} |u_{00}| &= \cos\theta_u, & |u_{10}| &= \sin\theta_u, & |v_{11}| &= \cos\theta_v, \\ |v_{01}| &= \sin\theta_v. \end{aligned} \quad (\text{D7})$$

The environment is initialized to a state of the form $\eta = \eta_0|0\rangle\langle 0| + (1 - \eta_0)|1\rangle\langle 1|$. The system and environment interact through a partial swap unitary given by $U_s = \sqrt{\tau}\mathbb{1} - i\sqrt{1 - \tau}\hat{S}$. After this interaction, a σ_x unitary is performed on the controller, before the system and controller interact again through U_s and the controller is traced out. For such a setup, the final output state is ρ_S^{out} , which does not depend on the value of η_0 and takes the form

We find that the Haar measure averaged fidelity is maximized when $\theta_u = \theta_v = \frac{\pi}{2}$, meaning that both U and V are equal to σ_x (up to a phase which does not affect the outcome). Plugging these optimal unitaries gives the maximum average output fidelity

$$A_{\text{MF}} = \frac{2}{3} - \frac{1}{3}\tau. \quad (\text{D8})$$

It is straightforward to see that this expression is lower than A_{CF} for all values of θ , except when $\tau = 1$ and there is no feedback present.

b. General POVMs

In the previous section, we considered MF using projective measurements in loop, but we can also consider more general POVMs. Here, we will consider the action of general POVMs in-between the two system-environment partial swap interactions. The polar decomposition can be used to write the Kraus operators of any POVM, represented with K_j as $K_j = U_j P_j$, where U_j is a unitary matrix and P_j is a positive-semidefinite matrix. Note that, to define a POVM, we must have $\sum_j K_j^\dagger K_j = \mathbb{1}$ which implies $\sum_k P_j^\dagger P_j = \mathbb{1}$. Thus, we can view any general POVM as the action of measurement characterized by $\{P_j\}$, followed by the action of a unitary U_j which depends on the measurement outcome (this observation was made in [6]). Since, in MF, we are already allowing for the action of a unitary depending on the measurement outcome, we can absorb U_j into these feedback unitaries and consider the measurement process as entirely characterized by $\{P_j\}$.

Furthermore, since our figure of merit is averaged over the Haar measure, which is unitarily invariant, we can assume that P_j are diagonal in the $\{|0\rangle, |1\rangle\}$ basis. Therefore, the most general qubit POVM can be described using the Kraus operators:

$$\begin{aligned} P_0 &= a|0\rangle\langle 0| + b|1\rangle\langle 1|, \\ P_1 &= \sqrt{1 - a^2}|0\rangle\langle 0| + \sqrt{1 - b^2}|1\rangle\langle 1| \end{aligned} \quad (\text{D9})$$

for $0 \leq a \leq 1$ and $0 \leq b \leq 1$. Note that when $a = b$, both elements of the POVM are proportional to the identity and correspond to no measurements being performed. When $a = 1$ and $b = 0$ the POVM corresponds to a projective measurement. Thus, the difference between a and b acts as a measure of the strength of the measurement.

We will absorb the action of U_j into U and V , so that the entire process is captured by a POVM with elements $\{UP_0, VP_1\}$.

Again, by using the decomposition of 2×2 unitary matrices, we come to the optimal protocol, which is when $U = V = \sigma_x$. Applying this optimal protocol yields the following expression for the Haar-measure averaged fidelity:

$$A_{\text{MF}} = \frac{1}{3}[\sqrt{1-a^2}\sqrt{1-b^2}(1-\tau) + ab(1-\tau) + 2-\tau]. \quad (\text{D10})$$

This expression yields the expression previously obtained for projective measurement feedback when $a = 1$ and $b = 0$. When $a = b = \frac{1}{2}$, we have $P_0 = P_1 = \frac{1}{2}\mathbb{1}$, which corresponds to no measurement being performed (or “infinitely weak” measurement) and only the action of the unitaries. In this case, (D10) yields the expression previously obtained for coherent feedback. It is in this sense CF can be viewed as MF in the limit of infinitely weak measurements.

It is straightforward to show that the output fidelity (D10) is maximized when $a = b$, thus proving that no measurement-based feedback process can outperform the coherent feedback protocol in this task. However, for performing a bit flip, POVMs corresponding to weaker measurements (where the value of a is closer to b) can achieve better performance than stronger measurements, as they disturb the input state less.

APPENDIX E: OPERATOR CONTROL IN THE LIMIT OF WEAK INTERACTIONS

We have looked at comparing MF and CF with a partial swap coupling

$$U_s^\theta = \cos \theta \mathbb{1} - i \sin \theta \hat{S}, \quad (\text{E1})$$

where \hat{S} is the full swap. When $\theta = 0$, both MF and CF are trivially the same, as the system and controller do not interact at all. We will now investigate the effect of MF and CF in the limit of an infinitesimal interaction angle $\theta \rightarrow d\theta$.

Expanding U_s to lowest order in θ ,

$$\lim_{\theta \rightarrow d\theta} U_s^\theta = \mathbb{1} - i d\theta \hat{S} + o[(d\theta)^2]. \quad (\text{E2})$$

Then, to first order we have

$$U_s U_T U_s = U_T - i d\theta \{S, U_T\} \quad (\text{E3})$$

for any operator U_T . The effect of one iteration of CF is

$$\rho \rightarrow \text{Tr}_C[U_s U_T U_s \rho \otimes \eta U_s^\dagger U_T^\dagger U_s^\dagger], \quad (\text{E4})$$

where $U_T = \mathbb{1} \otimes U$ is a unitary which acts only on the controller. Expanding U_s to first order in θ and discarding higher-order terms gives

$$\begin{aligned} \text{Tr}_C[U_T \rho \otimes \eta U_T^\dagger - i d\theta \{S, U_T\} \rho \otimes \eta U_T^\dagger \\ + i d\theta U_T \rho \otimes \eta \{S^\dagger, U_T^\dagger\}], \end{aligned} \quad (\text{E5})$$

Using the fact that $\text{Tr}_C(SA \otimes B) = \text{Tr}_C(BA)$ and the fact that the partial trace is cyclically invariant over the subspace which is being traced over, we obtain

$$\text{Tr}_C[\{S, U_T\} \rho \otimes \eta U_T^\dagger] = U \eta U^\dagger \rho + \eta \rho, \quad (\text{E6})$$

$$\text{Tr}_C[U_T \rho \otimes \eta \{S^\dagger, U_T^\dagger\}] = \rho U \eta U^\dagger + \rho \eta. \quad (\text{E7})$$

Combining these, we obtain the transformation

$$\rho_S \rightarrow \rho_S + i[\rho_S, U \eta U^\dagger] d\theta + i[\rho_S, \eta] d\theta. \quad (\text{E8})$$

To represent more general in-loop operations, we can replace U with a Kraus operator K_j acting on the controller. Due to the linearity of the trace, we can sum over these Kraus operators and in this way we obtain the expression

$$\rho_S \rightarrow \rho_S + i[\rho_S, \Phi(\eta)] d\theta + i[\rho_S, \eta] d\theta, \quad (\text{E9})$$

where $\Phi(\eta) = \sum_j K_j \eta K_j^\dagger$. This expression can be used to describe measurement-based feedback when K_j are used to describe the POVM operators, followed by the action of a unitary.

-
- [1] V. P. Belavkin, *Autom. Remote. Control* **44**, 178 (1983).
[2] H. M. Wiseman and G. J. Milburn, *Phys. Rev. A* **49**, 4110 (1994).
[3] H. M. Wiseman, *Phys. Rev. A* **49**, 2133 (1994).
[4] C. W. Gardiner and M. J. Collett, *Phys. Rev. A* **31**, 3761 (1985).
[5] S. Lloyd, *Phys. Rev. A* **62**, 022108 (2000).
[6] K. Jacobs, X. Wang, and H. M. Wiseman, *New J. Phys.* **16**, 073036 (2014).
[7] W. P. Smith, J. E. Reiner, L. A. Orozco, S. Kuhr, and H. M. Wiseman, *Phys. Rev. Lett.* **89**, 133601 (2002).
[8] C. Sayrin, I. Dotsenko, X. Zhou, B. Peaudecerf, T. Rybarczyk, S. Gleyzes, P. Rouchon, M. Mirrahimi, H. Amini, M. Brune, J.-M. Raimond, and S. Haroche, *Nature (London)* **477**, 73 (2011).
[9] H. M. Wiseman and G. J. Milburn, *Quantum Measurement and Control* (Cambridge University Press, Cambridge, 2009).
[10] A. Serafini, *ISRN Optics* **2012**, 275016 (2012).
[11] R. Hamerly and H. Mabuchi, *Phys. Rev. Lett.* **109**, 173602 (2012).
[12] S. Iida, M. Yukawa, H. Yonezawa, N. Yamamoto, and A. Furusawa, *IEEE Trans. Automat. Control* **57**, 2045 (2012).
[13] Z. Shi and H. I. Nurdin, *Quantum Inf. Comput.* **14**, 337 (2015).
[14] J. S. Bennett, L. S. Madsen, M. Baker, H. Rubinsztein-Dunlop, and W. P. Bowen, *New J. Phys.* **16**, 083036 (2014).
[15] Z. Wang and A. H. Safavi-Naeini, *Nat. Commun.* **8**, 15886 (2017).
[16] A. Harwood, M. Brunelli, and A. Serafini, *Phys. Rev. A* **103**, 023509 (2021).
[17] M. J. Woolley and A. A. Clerk, *Phys. Rev. A* **89**, 063805 (2014).
[18] J. Li, G. Li, S. Zippilli, D. Vitali, and T. Zhang, *Phys. Rev. A* **95**, 043819 (2017).
[19] N. L. Naumann, S. M. Hein, A. Knorr, and J. Kabuss, *Phys. Rev. A* **90**, 043835 (2014).
[20] J. Guo and S. Gröblacher, *Quantum* **6**, 848 (2022).
[21] G.-L. Schmid, C. T. Ngai, M. Ernzer, M. B. Aguilera, T. M. Karg, and P. Treutlein, *Phys. Rev. X* **12**, 011020 (2022).
[22] M. Hirose and P. Cappellaro, *Nature (London)* **532**, 77 (2016).

- [23] J. Zhang, R. Wu, Y. Liu, C. Li, and T. Tarn, *IEEE Trans. Automat. Control* **57**, 1997 (2012).
- [24] W.-L. Ma, S. Puri, R. J. Schoelkopf, M. H. Devoret, S. M. Girvin, and L. Jiang, *Sci. Bull.* **66**, 1789 (2021).
- [25] G. Crowder, L. Ramunno, and S. Hughes, *Phys. Rev. A* **106**, 013714 (2022).
- [26] H. I. Nurdin, M. R. James, and I. R. Petersen, *Automatica* **45**, 1837 (2009).
- [27] N. Yamamoto, *Phys. Rev. X* **4**, 041029 (2014).
- [28] C. Xiang, I. R. Petersen, and D. Dong, *Syst. Control Lett.* **141**, 104702 (2020).
- [29] Y. Liu, S. Shankar, N. Ofek, M. Hatridge, A. Narla, K. M. Sliwa, L. Frunzio, R. J. Schoelkopf, and M. H. Devoret, *Phys. Rev. X* **6**, 011022 (2016).
- [30] S. Whalen, A. Grimsmo, and H. Carmichael, *Quantum Sci. Technol.* **2**, 044008 (2017).
- [31] A. Harwood and A. Serafini, *Phys. Rev. Res.* **2**, 043103 (2020).
- [32] J. Rau, *Phys. Rev.* **129**, 1880 (1963).
- [33] L. Bruneau, A. Joye, and M. Merkli, *J. Math. Phys.* **55**, 075204 (2014).
- [34] V. Scarani, M. Ziman, P. Štelmachovič, N. Gisin, and V. Bužek, *Phys. Rev. Lett.* **88**, 097905 (2002).
- [35] F. Ciccarello, S. Lorenzo, V. Giovannetti, and G. M. Palma, *Phys. Rep.* **954**, 1 (2022).
- [36] S. Campbell and B. Vacchini, *Europhys. Lett.* **133**, 60001 (2021).
- [37] P. Strasberg, G. Schaller, T. Brandes, and M. Esposito, *Phys. Rev. X* **7**, 021003 (2017).
- [38] S. Lorenzo, A. Farace, F. Ciccarello, G. M. Palma, and V. Giovannetti, *Phys. Rev. A* **91**, 022121 (2015).
- [39] S. Lorenzo, R. McCloskey, F. Ciccarello, M. Paternostro, and G. M. Palma, *Phys. Rev. Lett.* **115**, 120403 (2015).
- [40] S. Seah, S. Nimmrichter, and V. Scarani, *Phys. Rev. E* **99**, 042103 (2019).
- [41] F. Ciccarello, *Quantum Meas. Quantum Metrol.* **4**, 53 (2017).
- [42] V. Giovannetti and G. Palma, *J. Phys. B: At. Mol. Opt. Phys.* **45**, 154003 (2012).
- [43] T. Rybár, S. N. Filippov, M. Ziman, and V. Bužek, *J. Phys. B: At., Mol. Opt. Phys.* **45**, 154006 (2012).
- [44] F. Ciccarello, G. M. Palma, and V. Giovannetti, *Phys. Rev. A* **87**, 040103(R) (2013).
- [45] S. Kretschmer, K. Luoma, and W. T. Strunz, *Phys. Rev. A* **94**, 012106 (2016).
- [46] L. Bouten, R. van Handel, and M. R. James, *SIAM Rev.* **51**, 239 (2009).
- [47] A. Pechen, N. Il'in, F. Shuang, and H. Rabitz, *Phys. Rev. A* **74**, 052102 (2006).
- [48] C. Shen, K. Noh, V. V. Albert, S. Krastanov, M. H. Devoret, R. J. Schoelkopf, S. Girvin, and L. Jiang, *Phys. Rev. B* **95**, 134501 (2017).
- [49] V. Jurdjevic and H. J. Sussmann, *J. Diff. Equ.* **12**, 313 (1972).
- [50] S. G. Schirmer, I. C. Pullen, and A. I. Solomon, *IFAC Proc. Vol.* **36**, 281 (2003).
- [51] F. Albertini and D. D'Alessandro, *IEEE Trans. Automat. Control* **48**, 1399 (2003).
- [52] D. D'Alessandro, *Introduction to Quantum Control and Dynamics* (CRC Press, Boca Raton, FL, 2021).
- [53] D. Dong and I. R. Petersen, *IET Control. Theory Appl.* **4**, 2651 (2010).
- [54] S. G. Schirmer and A. I. Solomon, in *Proceedings ICCSUR 8: 8th Int'l Conference on Squeezed States and Uncertainty relations* (Rinton Press, Princeton, NJ, 2003).
- [55] T. M. Karg, B. Gouraud, P. Treutlein, and K. Hammerer, *Phys. Rev. A* **99**, 063829 (2019).
- [56] N. K. Bernardes, A. Cuevas, A. Orioux, C. H. Monken, P. Mataloni, F. Sciarrino, and M. F. Santos, *Sci. Rep.* **5**, 17520 (2015).
- [57] C. Marletto, V. Vedral, L. Knoll, F. Piacentini, E. Bernardi, A. Avella, M. Gramegna, I. P. Degiovanni, E. Rebufello, and M. Genovese, *Phys. Rev. Lett.* **128**, 080401 (2022).
- [58] D. Cilluffo, A. Carollo, S. Lorenzo, J. A. Gross, G. M. Palma, and F. Ciccarello, *Phys. Rev. Res.* **2**, 043070 (2020).
- [59] A. Carollo, D. Cilluffo, and F. Ciccarello, *Phys. Rev. Res.* **2**, 043184 (2020).
- [60] M. V. Gustafsson, T. Aref, A. F. Kockum, M. K. Ekström, G. Johansson, and P. Delsing, *Science* **346**, 207 (2014).
- [61] B. Kannan, M. J. Ruckriegel, D. L. Campbell, A. Frisk Kockum, J. Braumüller, D. K. Kim, M. Kjaergaard, P. Krantz, A. Melville, B. M. Niedzielski, A. Vepsäläinen, R. Winik, J. L. Yoder, F. Nori, T. P. Orlando, S. Gustavsson, and W. D. Oliver, *Nature (London)* **583**, 775 (2020).
- [62] X. Gu, A. F. Kockum, A. Miranowicz, Y.-xi Liu, and F. Nori, *Phys. Rep.* **718-719**, 1 (2017).
- [63] H. Nakazato, T. Takazawa, and K. Yuasa, *Phys. Rev. Lett.* **90**, 060401 (2003).
- [64] J. Gough and M. R. James, *IEEE Trans. Automat. Control* **54**, 2530 (2009).
- [65] H. I. Nurdin and J. E. Gough, *Quantum Inf. Comput.* **15**, 1017 (2015).
- [66] R. McCloskey and M. Paternostro, *Phys. Rev. A* **89**, 052120 (2014).
- [67] S. Campbell, M. Popovic, D. Tamascelli, and B. Vacchini, *New J. Phys.* **21**, 053036 (2019).
- [68] K. Audenaert, N. Datta, and M. Ozols, *J. Math. Phys.* **57**, 052202 (2016).
- [69] E. A. Carlen, E. H. Lieb, and M. Loss, *J. Math. Phys.* **57**, 062203 (2016).
- [70] S. Lloyd, *Phys. Rev. A* **56**, 3374 (1997).
- [71] N. Shiraishi, S. Ito, K. Kawaguchi, and T. Sagawa, *New J. Phys.* **17**, 045012 (2015).
- [72] G. Schaller, J. Cerrillo, G. Engelhardt, and P. Strasberg, *Phys. Rev. B* **97**, 195104 (2018).
- [73] B.-L. Najera-Santos, P. A. Camati, V. Métillon, M. Brune, J.-M. Raimond, A. Auffèves, and I. Dotsenko, *Phys. Rev. Res.* **2**, 032025(R) (2020).
- [74] N. Freitas and M. Esposito, *Phys. Rev. E* **103**, 032118 (2021).
- [75] S. Lloyd, *Phys. Rev. Lett.* **75**, 346 (1995).
- [76] P. Rouchon, *Annu. Rev. Control* **54**, 252 (2022).
- [77] A. Serafini, *Quantum Continuous Variables: A Primer of Theoretical Methods* (CRC Press, Boca Raton, FL, 2017).